Spatial variability of soil respiration (Rs) and its controls are subjected to strong seasonality in an even-aged European beech (Fagus sylvatica L.) stand

SCHOLARONE™
Manuscripts

292x93mm (150 x 150 DPI)

320x284mm (150 x 150 DPI)
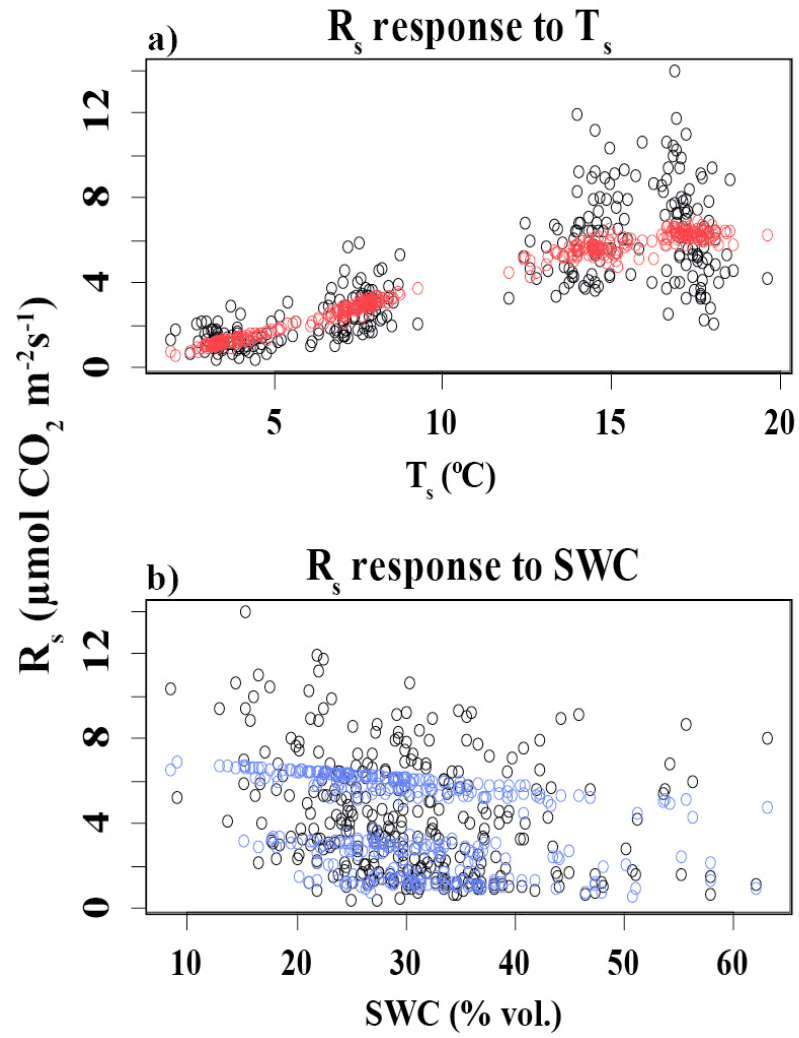
143x200mm (150 x 150 DPI)
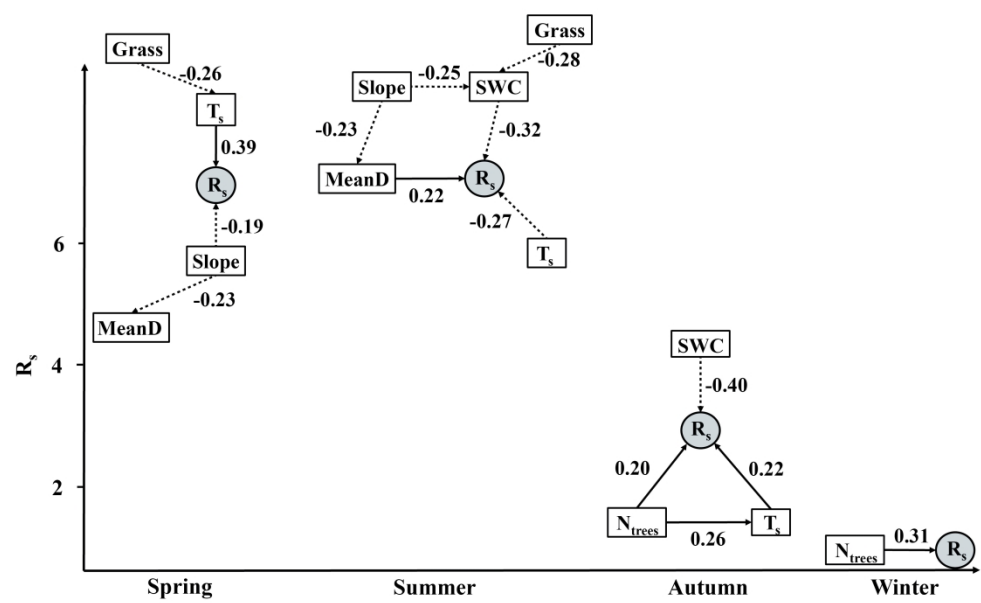
622x376mm (150 x 150 DPI)
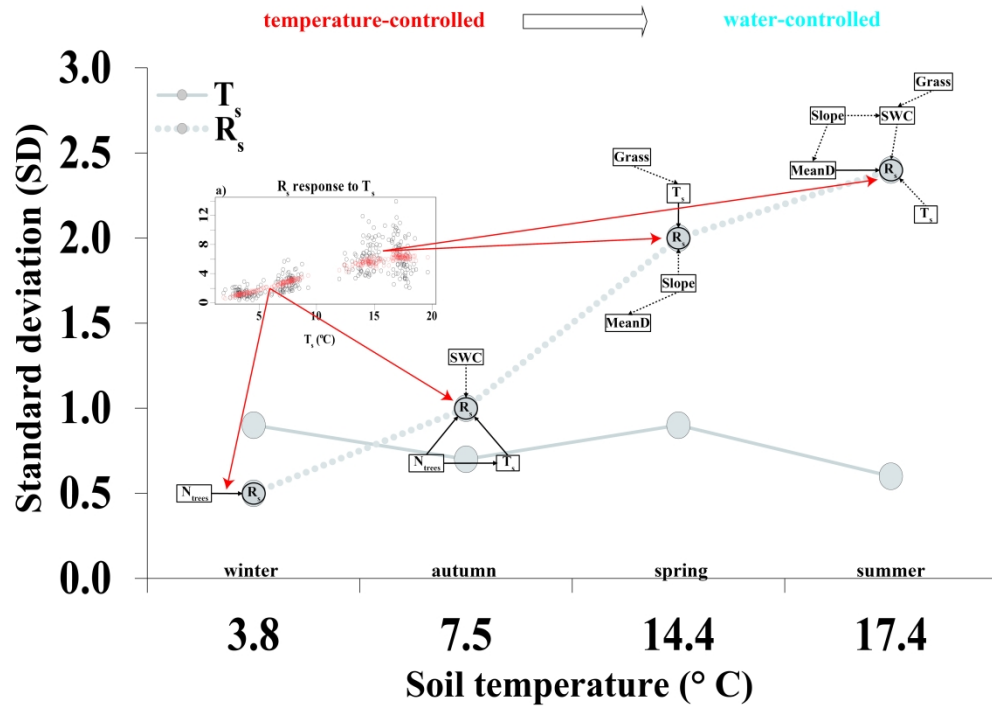
1046x735mm (150 x 150 DPI)
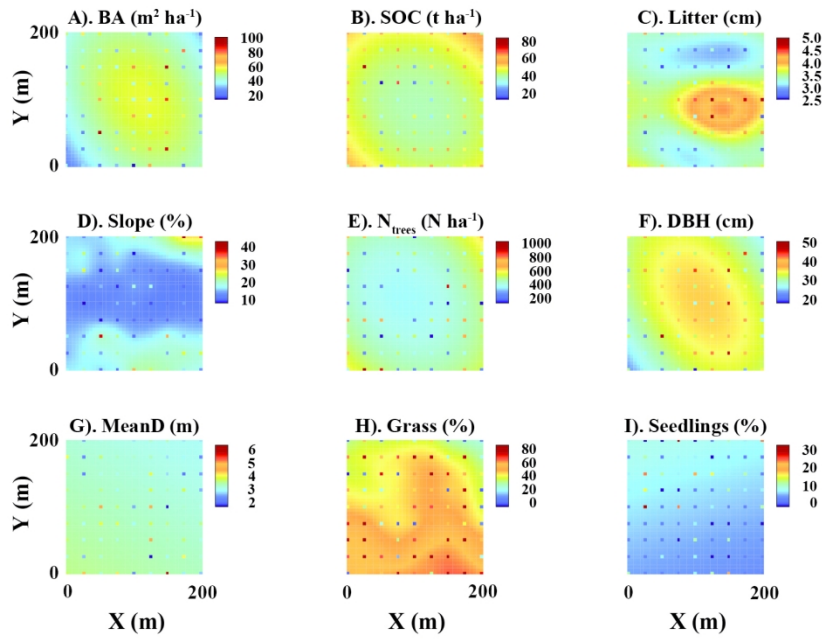
320x219mm (150 x 150 DPI)

1   **Spatial variability of soil respiration (R$_s$) and its controls are subjected to strong**

2   **seasonality in an even-aged European beech (*Fagus sylvatica* L.) stand**

3

4   **Running Title:** Space-Time R$_s$ variability in European beech stand

5

6   **Authors**: Hereş Ana-Maria[1,2], Bragă Cosmin[3], Petritan Any Mary[3], Petritan Ion Catalin[4], Curiel

7   Yuste Jorge[2,5,*]

8

9   [1]Transilvania University of Braşov, Faculty of Silviculture and Forest Engineering, Department

10   of Forest Sciences, Șirul Beethoven -1, 500123, Braşov, Romania

11

12   [2]BC3 - Basque Centre for Climate Change, Scientific Campus of the University of the Basque

13   Country, 48940 Leioa, Spain

14

15   [3]National Institute for Research and Development in Forestry "Marin Drăcea", Bulevardul

16   Eroilor 128, 077190, Voluntari, Romania

17

18   [4]Transilvania University of Braşov, Faculty of Silviculture and Forest Engineering, Department

19   of Forest Engineering, Forest Management Planning and Terrestrial Measurements, Șirul

20   Beethoven -1, 500123, Braşov, Romania

21

22   [5]IKERBASQUE - Basque Foundation for Science, Plaza Euskadi 5, 48009, Bilbao, Spain

23

24   * Corresponding author:

25   Dr. Jorge Curiel Yuste

26   Ikerbasque Research Professor

27   BC3 - Basque Centre for Climate Change, Sede Building 1, 1st floor, Scientific Campus of

28   the University of the Basque Country, 48940 Leioa

29   Email address: jorge.curiel@bc3research.org

30   Contact phone: +34 94-401 46 90 ext. 179

31 **Keywords:** European beech, even-aged stand, micro-topography, seasonality, soil
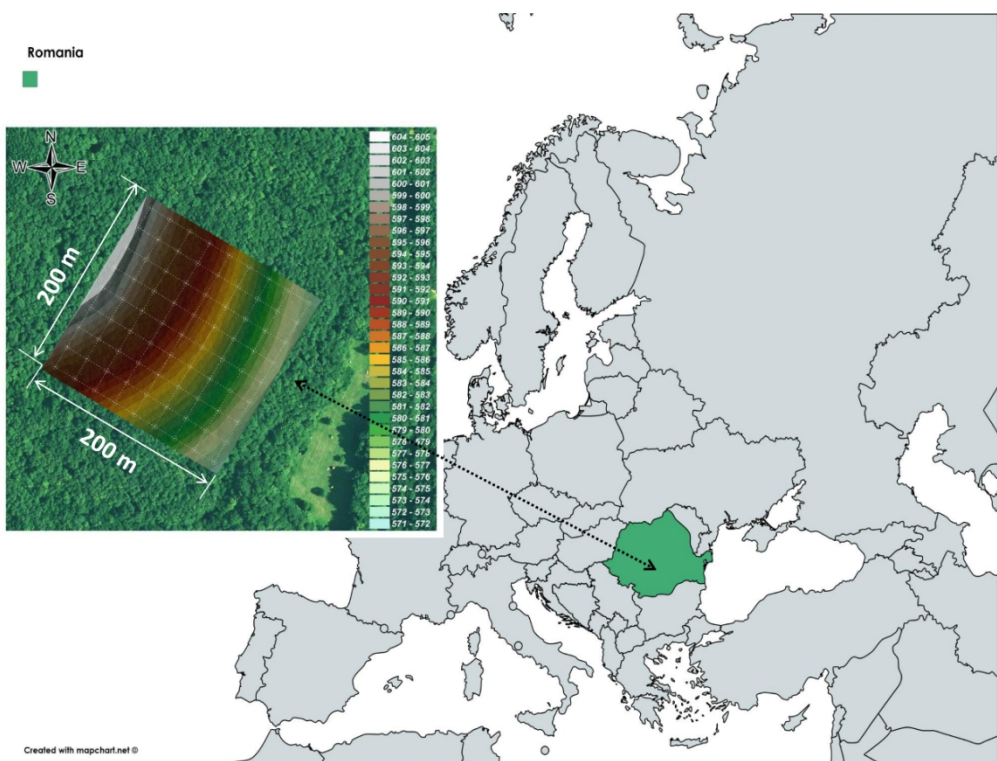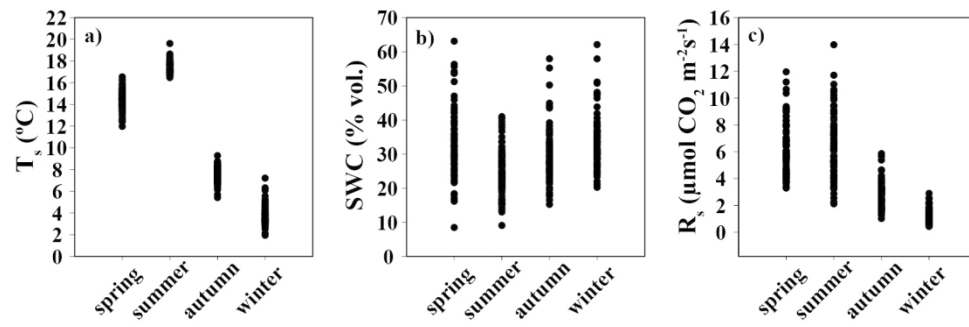
32 microclimate, soil respiration, spatial variability

33

34 **Abbreviations: R_s,** soil respiration; **T_s,** soil temperature; **SWC,** soil water content; **BA,** basal

35 area of the European beech trees surrounding the 81 measurement points; **SOC,** soil organic

36 carbon content; **Litter,** thickness of the litter layer; **Slope,** micro-topography of the terrain

37 within the study stand; **N_{trees},** the count of all the surrounding European beech trees around each

38 of the 81 measurement points; **DBH,** average diameter at breast height (i.e., > 6 cm) of the

39 European beech trees surrounding the 81 measurement points; **MeanD,** mean distance from the

40 European beech trees to the 81 measurement points; **Grass,** percentage of the soil surface

41 covered by grass; **Seedlings,** percentage of the soil surface covered by tree seedlings.

42   **Abstract**

43

44   Uncertainties arising from the so far poorly explained spatial variability of soil respiration (R_s)

45   remain large. This is partly due to the limited understanding on how actually spatially variable

46   R_s is, but also on how environmental controls determine R_s's spatial variability and how these

47   controls vary in time (e.g., seasonally). Our study was designed to deepen into the complexity

48   of R_s's spatial variability in a European beech even-aged stand, covering both phenologicaly

49   and climatically contrasting periods (spring, summer, autumn, winter). Although we studied a

50   relatively homogenous stand, we found a large spatial variability of R_s (coefficients of variation

51   > 30%) characterized by strong seasonality. This large spatial variability of R_s suggests that

52   even in relatively homogenous stands there is a large potential source of error when estimating

53   R_s. This was also reflected by the sampling effort needed to obtain seasonal robust estimates of

54   R_s, which may actually require a number of samples above that used in R_s studies. We further

55   postulate that the effect of seasonality on the spatial variability and environmental controls of

56   R_s was determined by the seasonal shifts of its microclimatic controls: during winter, low

57   temperatures constrain plant and soil metabolic activities and hence reduce R_s variability

58   (temperature-controlled processes), while during summer, water demand by vegetation and

59   changes in water availability due to the micro-topography of the terrain (i.e., slope) increase R_s

60   variability (water-controlled processes). This study provides novel information on the spatio-

61   temporal variability of R_s and deepens into the seasonality of its environmental controls and the

62   architecture of their causal-effect relationships controlling R_s's spatial variability. Our study

63   further shows that improving current estimates of R_s at local and regional levels might be

64   necessary in order to reduce uncertainties and improve CO_2 estimates at larger spatial scales.

65

66   **Highlights**

67

68   ❖ The spatial variability of soil respiration (R_s) and its environmental controls vary

69   seasonally

70   ❖ Seasonal shifts from temperature- to water-controlled processes determine R_s's spatial

71   variability

72   ❖ Besides microclimate, slope and grass cover explain the spatio-temporal variability of

73   R_s

74   ❖ An intense sampling effort is needed to obtaining robust R_s estimates even in

75   homogenous forests

76

77   **1. Introduction**

78

79   Soil respiration (R_s), i.e., the production and subsequent emission of carbon dioxide (CO_2) from

80   the soil to the atmosphere, is one of the key processes contributing to the global terrestrial

81   carbon (C) balance/budget. R_s is mainly produced by biological sources from the aerobic

82   respiration of decomposers (i.e., heterotrophic respiration), as well as by plant roots and

83   associated microorganisms living in the rhizosphere (i.e., autotrophic respiration) (Rodeghiero

84   & Cescatti, 2008), but also by non-biological chemical oxidation reactions of C in organic

85   matter, although at lower rates in this latter case (Raich & Schlesinger, 1992). Globally, the R_s

86   emissions amount to a total of almost 80 PgC y^{-1}, being the second largest C flux after CO_2

87   uptake by plants (Raich & Tufekciogul, 2000), which means more than half of an ecosystem's

88   total CO_2 emissions come from R_s (Barba et al., 2018; Curiel Yuste et al., 2005; Janssens et al.,

89   2001). However, R_s is also probably the least well understood part of the C budget at global

90   terrestrial ecosystems' level, based primarily on the fact that the large spatio-temporal

91   variability that characterizes this large flux requires of a substantial monitoring effort at

92   different scales and hence, of a large investment in instrumentation for its correct monitoring

93   (Bond-Lamberty & Thomson, 2010). Therefore, and despite the large critical mass of studies

94   performed to understand it (Bond-Lamberty & Thomson, 2010), our knowledge on the

95   mechanisms controlling this large flux remains very limited (e.g., Barba et al., 2013; Curiel

96   Yuste et al., 2019). Hence, there is still a need for studies designed to explore the spatio-

97   temporal variability of R_s in order to be able to calibrate models and improve predictions of soil

98   biological CO_2 emissions in a changing environment.

99

100   The magnitude of R_s-related CO_2 emissions varies in time and space depending on multiple

101   drivers. A critical mass of studies has been designed to understand how the temporal variability

102   of R_s relates to different environmental factors such as soil temperature (T_s; e.g., Chen et al.,

103   2014; Davidson et al., 1998; Epron et al., 2004*a*), soil water content (SWC; e.g., Davidson et

104   al., 2000; Oishi et al., 2013; Poblador et al., 2017), wind (e.g., Sánchez-Cañete et al., 2016), or

105   the photosynthetic activity of the plants (e.g., Bahn et al., 2009; Curiel Yuste et al., 2005;

106   Davidson et al., 1998). Nevertheless, it is important to highlight the discrepancy between the

107   large number of studies undertaken to understand the large, but predominantly explained

108   variability in time (generally seasonal) of soil CO_2 fluxes (see for instance Bond-Lamberty &

109   Thomson, 2010) and the relatively few studies undertaken to understand the enormous, but

110   largely unexplained spatial variability of this very same flux. Several studies have proposed

111   different factors that define local conditions as controls of the spatial variability of R_s at the

112   mesoscale (scale of m). Most of these studies agree on the important role of variables such as:

113   *i*). the spatial variability of soil moisture (Barba et al., 2013; Kosugi et al., 2007; Poblador et

114   al., 2017); *ii*). the structure of the overstorey plant community (Barba et al., 2013; Epron et al.,

115   2004*b*; Law et al., 2001; Saiz et al., 2006; Søe & Buchmann, 2005); *iii*). variables directly

116   related to the structure of the aboveground plant community, such as leaf production (Oishi et

117   al., 2013), root density or biomass (Knohl et al., 2008), microbial biomass, and litter thickness

118   (Hanson et al., 1993); *iv*). the quantity and quality of soil organic matter (Rayment & Jarvis,

119   2000); or *v*). the C/N ratio and bulk density of the top soil (Khomik et al., 2006; Ngao et al.,

120   2012; Saiz et al., 2006). Other topographical aspects, such as the slope and the position within

121   the landscape, have been however less studied although their contribution to explain the spatial

122   variability of R_s might also be critical (Arias-Navarro et al., 2017; Berryman et al., 2015; Brito

123   et al., 2010; Hanson et al., 1993; Riveros-Iregui et al., 2012;). All studies, nevertheless,

124   conclude that our capacity to predict the spatial variability of R_s and its environmental controls

125   remains largely insufficient (e.g., Allaire et al., 2012).

126

127   The environmental controls of the spatial variability of R_s may also vary temporally, though, to

128   the best of our knowledge, only few studies have been designed to deepen in this potential

129   temporal axis of the spatial variation of R_s (Epron et al., 2004*b*; Khomik et al., 2006; Kosugi et

130   al., 2007; Saiz et al., 2006; Shi et al., 2016; Søe & Buchmann, 2005). The complexity of the

131   spatial variability of R_s can vary seasonally (Riveros-Iregui et al., 2012; Shi et al., 2016; Søe &

132   Buchmann, 2005) specially because different environmental drivers may differently influence

133   R_s depending on the season. For instance, the influence of water availability on the spatial

134   patterns of R_s at the landscape-scale can exhibit a bidirectional behaviour, R_s being more

135   sensitive to water availability during dry periods or in highly drained areas than during wetter

136   periods or in low drainage areas (Riveros-Iregui et al., 2012). Likewise, the biomass and

137   respiration of the autotrophic (roots and rhizosphere microorganism) and heterotrophic

138   (microbial activity) components of R_s may vary in space and time depending on the

139   phenological state of the vegetation and its nutrient and water demands (Barba et al., 2013; Søe

140   & Buchmann, 2005). For this reason, understanding the drivers controlling the spatial

141   variability of R_s at different temporal scales may help us to improve and modulate the sampling

142   effort needed in order to obtain confident estimates of R_s. This also means that obtaining reliable

143   integrative measures of R_s would require different sampling efforts throughout the year. It is,

144   therefore, important to understand this seasonally-dependent complexity if we want to improve

145   our knowledge on the sampling effort needed to get accurate and costly efficient estimates of

146   R_s (Barba et al., 2013; Herbst et al., 2009; Rayment & Jarvis, 2000; Rodeghiero & Cescatti,

147   2008).

148

149   We studied the spatio-temporal variability of soil respiration (R_s) in a 4.0 ha (i.e., 200 m x 200

150   m) European beech (*Fagus sylvatica* L.) even-aged stand. Specifically, we focused on

151   understanding the potential seasonal (i.e., spring, summer, autumn, winter) variations of R_s and

152   its environmental controls to: (1) determine the magnitude of their spatial variability and the

153   sampling effort needed per each season (i.e., spring, summer, autumn, winter) to obtain robust

154   average estimates of R_s; and (2) identify the main environmental controls and the architecture

155   of their potential causal-effect relationships controlling the spatial variability of R_s along the

156   seasons (i.e., during phenologically and climatically contrasted periods of the year). We

157   hypothesized that, given the generally large influence of the aboveground plant distribution in

158   explaining the spatial variability of R_s, the spatial variability of R_s will be low in our European

159   beech even-aged study stand where trees are homogeneously distributed (H1). However, we

160   also hypothesized that, along with other already well-studied and known factors, other factors

161   (i.e., more spatially variable at stand level), such as the micro-topography of the terrain (i.e.,

162   slope) or the spatial distribution of the grass cover, will also play an important, indirect control

163   over R_s due to their influence on the spatial variability of the soil water content (SWC) (H2).

164   Finally, we also hypothesized that the predictive power of the different environmental controls

165   of the spatial variability of R_s will vary throughout the year depending on the environmental

166   constrains that act on R_s within a given season (e.g., soil temperature, T_s; or soil water content,

167   SWC) (H3).

168

169   **2. Materials and Methods**

170

171   *2.1.   Study site and stand*

172

173   The study site (i.e., forest) is located in the central-southern part of Romania, in Mihaesti (Arges

174   county; 45°05'11.8019"N, 25°03'58.0428"E), at an altitude of 570 m a.s.l. (Figure 1). This forest

175   is largely dominated by European beech, although other tree species may also be found:

176   hornbeam (*Carpinus betulus* L.)*,* sessile oak *(Quercus petraea* (Matt.) Liebl.), or sweet cherry

9

177 *(Prunus avium L.)*. The density within the whole forest located in Mihaesti is of 504 trees ha^{-1},

178 with a total volume of 502 m^3 ha^{-1}, and a basal area of 33 m^2 ha^{-1} (Mihaesti Forest Management

179 Plan). Within this forest, we focused on a 4.0 ha European beech study stand (200 m x 200 m)

180 (Figure 1). The European beech trees within the study stand are mainly adult and dominant (i.e.,

181 canopy level). According to the Mihaesti Forest Management Plan, most individuals within the

182 study stand have an estimated age of ~ 85 years, which allows us to consider this study stand

183 as being even-aged. The area where our study stand is located is characterized by a temperate

184 continental climate, with a mean annual precipitation of ~ 875.21 mm, and a mean air

185 temperature of ~ 6.31°C, respectively (estimates calculated for the 1901 – 2019 period; CRU

186 TS v.4; Harris et al., 2020). The mean annual precipitation for 2016 and 2017 (i.e., the years

187 when our measurements were performed; see below) was of ~ 991.80 mm and ~ 959.60 mm,

188 respectively. As for the mean annual air temperature, it was of ~ 7.59 °C in 2016 and of 7.54

189 °C in 2017 (CRU TS v.4; Harris et al., 2020). The soils are Eutric Cambisols (clay loam)

190 covered with mull type humus, developed on a sandstone with marls parental material (Florea

191 & Munteanu, 2012). The slope within the study stand is smooth and there are no important

192 differences regarding the altitude between the upper part of the study stand and the lower part

193 of the study stand (Figure 1, small panel). Mean pH values range from 4.8 (0-10 cm soil depth)

194 to 5.2 (11-20 cm soil depth) (WTW pH330i; WTW GmbH, Weilheim, Germany).

195

196   *2.2.*   *Field soil respiration (R_s) and microclimatic factors measurements*

197

198 The 4.0 ha selected study stand was divided into regular 25 m x 25 m squares (Figure 1, small

199 panel). Soil respiration (R_s) measurements were then performed at each of the four corners of

200 each of the 25 m x 25 m squares, resulting thus on a total of 81 measurement points. R_s

201 measurements were all performed using a Portable Infrared Gas Analyzer (IRGA) connected to

202   a soil respiration standard chamber (EGM-4 and SRC-1; PP Systems, Amesbury, MA, USA).

203   The soil respiration chamber covered a soil surface area of 78 cm^2 and an enclosed volume of

204   1171 cm^3. Since some studies have shown a clear correlation between insertion depth, the

205   amount of cut roots, and the lost soil effluxes (Silvola et al., 1996; Wang et al., 2005), no collars

206   were inserted in the soil (Arias-Navaro et al., 2017; Epron et al., 2004*b*; Hanson et al., 1993;

207   Maestre & Cortina, 2003; Poblador et al., 2017). Instead, we followed a similar procedure to

208   the one described by Epron et al., 2004*b* and we inserted the edge of the respiration chamber to

209   a depth of 1 cm into the soil, including the litter layer. Nevertheless, this was done only after

210   firstly removing the herbaceous layer in order to avoid potential confounding effects of the

211   vegetation on R_s measurements. Furthermore, to avoid potential gas leaks due to the shallow

212   insertion of the respiration chamber (1 cm into the soil) with respect to a relatively thick low-

213   density litter layer (average 3.3 cm; Table 1), the respiration chamber was strongly pressed

214   against the soil (i.e., with the help of one hand) over the whole time measurements were

215   performed. Final R_s values were estimated for 120 seconds based on the linear increase of the

216   CO_2 concentration within the soil respiration chamber (i.e., a closed dynamic system). Soil CO_2

217   efflux measurements were always performed between 9 a.m. and 5 p.m. Additionally, the CO_2

218   effluxes were never measured during rainy days. Specifically, in case of heavy rains (i.e., > 15

219   mm), field R_s measurements were postponed 36 h to avoid the "Birch effect" (Birch, 1958).

220

221   Simultaneously to the field R_s measurements, microclimatic measurements (i.e., soil

222   temperature and the volumetric soil water content) were also performed at the same 81

223   measurement points. Specifically, soil temperature (T_s) was measured at 5 cm soil depth using

224   the STP-2 Soil Temperature Probe that was attached to the IRGA (PP Systems, Amesbury, MA,

225   USA). As for the volumetric soil water content (SWC), this variable was measured at 20 cm

226   soil depth using the TDR 300 soil moisture meter (Spectrum Technologies, Inc., Plainfield, IL,

227   USA). All field measurements (i.e., R_s, T_s, and SWC) spanned over a period of one complete

228   year and thus over the four seasons: spring (May 2016), summer (August 2016), autumn

229   (November 2016), and winter (February 2017). Within each of the 4 seasons and at each of the

230   81 measurement points, we performed 3 independent measurements for each of the 3 variables

231   (i.e., R_s, T_s, and SWC) and then averaged their corresponding values. In order to systematically

232   perform R_s, T_s, and SWC measurements at exactly the same locations within the study stand,

233   we marked the 81 measurement points with wood sticks that were maintained in their positions

234   over the whole study period. Due to the large number of measurement points (i.e., 81) and thus

235   to the considerable field effort and logistics that were needed, R_s, T_s, and SWC measurements

236   were always performed during 2 consecutive days during each season.

237

238   *2.3.   Forest structural and soil variables and the micro-topography of the terrain*

239

240   At each of the 81 measurement points, soil samples were also collected to determine the soil

241   organic carbon (SOC) content. All soil samples were collected in February 2017 after all

242   seasonal measurements (i.e., R_s, T_s, and SWC) were finished. Soil sampling was performed

243   using a metallic cylinder (5 cm diameter, and 20 cm depth) and consisted in extracting one soil

244   core at each of the 81 measurement points. SOC of the upper 20 cm of the soil profile was

245   determined through the dry combustion method using a CHNS organic elemental micro-

246   analyser (TruSpec Micro CHNS elemental analyser, LECO, New York, USA).

247

248   The thickness of the litter layer (hereinafter referred to as "litter" to simplify) was used as a

249   proxy of litter biomass, which could not be measured due to logistics. The litter, at each of the

250   81 measurement points, was measured only once during the 2016 summer, two weeks before

251   the R_s, T_s, and SWC measurements started. Although, we acknowledge the fact that it would

252 have been better to measure the litter layer over the year (i.e., seasons), this was not possible

253 due to logistics. Instead, we assumed that the place where there was more accumulated litter

254 (i.e., at some point) would be the same place where more litter usually falls and the opposite

255 for the places where there was less accumulated litter. Accordingly, the litter depth would be

256 basically stable over the year (i.e., seasons). Simultaneously to the litter measurements, the

257 micro-topography of the terrain (hereinafter referred to as "slope" to simplify), at each of the

258 81 measurement points, was also measured.

259

260 In order to account for the impact of the surrounding vegetation on our field measurements (i.e.,

261 within a radius of 7 m around each of the 81 measurement points), we counted all the

262 surrounding European beech trees (N_{trees}) and we measured their diameter at breast height

263 (DBH; at standard 1.3 m above from the ground) and their distance to the 81 sampling points.

264 The 7 m radius was established considering the average crown diameter of the European beech

265 trees found within the 4.0 ha study stand (Mihaesti Forest Management Plan). The DBH of the

266 trees was measured using a calliper (Haglöf, Sweden), only European beech trees with a DBH

267 > 6 cm being finally considered for this study. The measured distances were used to calculate

268 the mean distances (MeanD) from surrounding European beech trees to the 81 measurement

269 points. In order to estimate the basal area (BA; m^2 ha^{-1}) of all European beech trees with a DBH

270 > 6 cm, we calculated the sum of all their cross-sectional areas at breast height. Finally, within

271 the same radius of 7 m around each of the 81 measurement points, we also estimated the

272 percentage (%) of the soil surface covered by grass and the percentage (%) of the soil surface

273 covered by all tree seedlings. These estimations were done visually and agreed between several

274 observers for data consistency.

275

276   *2.4.   Statistical analyses*

13

277

278   We used different statistics (i.e., mean, M; standard deviation, SD; and relative variability, RV)

279   to estimate relative rates of spatial variability of forest structural and soil variables (i.e., BA,

280   SOC, litter, N_{trees}, DBH, MeanD, % of grass, and % of seedlings) and of the micro-topography

281   of the terrain (i.e., slope). We used the same statistics (i.e., mean, M; standard deviation, SD;

282   and relative variability, RV) plus the absolute amplitude (A; defined as the difference between

283   maximum and minimum values) to estimate relative and absolute rates of spatial variability of

284   the microclimate (i.e., T_s and SWC) and soil respiration (R_s) variables. As most studies give the

285   coefficient of variation (CV), we also calculated this statistic (i.e., expressed as a percentage)

286   for the R_s variable alone and used it to compare our results with those published in previous

287   studies. For the T_s, SWC, and R_s variables, all the above mentioned statistics were calculated

288   considering both the four seasons separately and the four seasons combined (i.e., annual). The

289   relative variability statistic (i.e., RV) was calculated following Lewontin 1966 and Webster

290   2001 as the standard deviation of the logarithms (i.e., log10 in our case) of measurements.

291   Relative variability allows thus to compare variations between different groups of observations

292   (Lewontin 1966; Webster 2001).

293

294   In order to calculate the minimum number of measurements (i.e., N) needed to obtain robust

295   estimates of R_s for each season (i.e., spring, summer, autumn, and winter), we used the

296   following power equation (Davidson et al., 2002):

297

298                    $$N = [(t \times s)/(range/2)]^2 \qquad\qquad equation\ 1$$

299

300   where, t is represented by the critical value of the t-distribution (two-tailed test) for a given

301   confidence level (99, 95, and 90%, respectively) and for 80 degrees of freedom; s is the standard

302 deviation of all spatially independent R_s measurements per each season (i.e., spring, summer,

303 autumn, and winter); and *range* is the width of the desired interval around the mean of the R_s

304 measurements of each season (i.e., spring, summer, autumn, and winter) in which a smaller

305 sample mean is expected to fall (i.e., error limit of 10%, 20%, and 30% of the R_s measurements

306 mean per each season).

307

308 We run geostatistical analyses (i.e., experimental (semi-) variograms and theoretical

309 variograms) to determine the spatial autocorrelation of: *i*). the T_s, SWC, and R_s variables,

310 separately for each season (i.e., spring, summer, autumn, and winter); *ii*). all forest structural

311 and soil variables (i.e., basal area, BA; soil organic carbon content, SOC; thickness of the litter

312 layer, litter; number of trees surrounding the 81 measurement points, N_{trees}; diameter at breast

313 height, DBH; mean distance from surrounding European beech trees to the 81 measurement

314 points, MeanD; percentages of grass and seedlings cover around the 81 measurement points);

315 and *iii*). the micro-topography of the terrain (i.e., slope). Specifically, the experimental (semi-)

316 variograms (i.e., binned) were performed using the "variog" function available from the "geoR"

317 R package (Ribeiro et al., 2020) based on classical estimators. Further on, the theoretical

318 variograms were performed using the "likfit" function available from the "geoR" R package

319 (Ribeiro et al., 2020). These analyses were run considering the restricted maximum likelihood

320 (REML) parameter estimation, different trends (i.e., the mean part of the model; constant, first

321 order polynomial, and second order polynomial), and functions (i.e., models for the correlation

322 function; matern, exponential, Gaussian, spherical, circular, cubic, wave, powered exponential,

323 Cauchy, gneiting, and pure nugget). A total of 693 models were run. The selection of the best

324 models for each of the analysed variables was based on AIC (Akaike Information Criteria). The

325 selected models were then used to perform ordinary kriging using the "krige.conv" function

326 available from the "geoR" R package (Ribeiro et al., 2020). The "image" function available

15

327 from the "geoR" R package (Ribeiro et al., 2020) was finally used to visualize the spatial

328 prediction based on the fixed covariance parameters. All selected models were validated using

329 the "xvalid" function available from the "geoR" R package (Ribeiro et al., 2020).

330

331 To evaluate the microclimatic controls of the spatio-temporal variability of R_s, we run multiple

332 regression functions using the "nls" function available from the "MASS" R package (Venables

333 & Ripley, 2020). These functions were designed according to literature (i.e., Vicca et al., 2014).

334 Briefly, different models were designed to represent the independent controls of soil

335 temperature (T_s) and soil water content (SWC) on R_s, but also taking into account potential

336 unimodal responses of R_s to both microclimatic factors. R_s data was log transformed prior to

337 analyses as it did not meet the normality assumption.

338

$$\log(R_s) \sim a + b*T_s \qquad\qquad \textit{equation 2}$$

$$\log(R_s) \sim a + b*SWC \qquad\qquad \textit{equation 3}$$

$$\log(R_s) \sim a + b*T_s + c*T_s^2 \qquad\qquad \textit{equation 4}$$

$$\log(R_s) \sim a + b*SWC + c*SWC^2 \qquad\qquad \textit{equation 5}$$

$$\log(R_s) \sim a + b*T_s + c*SWC \qquad\qquad \textit{equation 6}$$

$$\log(R_s) \sim a + b*T_s + c*SWC + d*T_s^2 \qquad\qquad \textit{equation 7}$$

$$\log(R_s) \sim a + b*T_s + c*SWC + d*SWC^2 \qquad\qquad \textit{equation 8}$$

339

340 Where, *a*, *b*, *c*, and *d* letters stand for coefficients of the multiple regression functions. The co-

341 variance and multicollinearity between T_s and SWC were examined prior to analyses using the

342 Variance Inflation Factor (VIF). Since the VIF was lower than 2, both microclimatic variables

343 could be used within the same model (Zuur et al., 2010). The selection of the best model was

344 based on the AIC (Akaike Information Criterion). For these analyses, the T_s, SWC, and R_s

345 variables were combined over the four seasons (i.e., spring, summer, autumn, and winter). All

346 these analyses were conducted based on the assumption that the residuals of the models were

347 normally distributed ($p > 0.05$) and independent. As the assumption of independence may be

348 justified when data collection has been performed based on a probability sampling design (e.g.,

349 de Gruijter et al., 2006) and our data collection has been performed based on a grid sampling

350 design, we acknowledge the fact that the spatial auto-correlation between data at nearby

351 measurement points might impact some of the obtained results.

352

353 To describe potential complex causal-effect relationships that might determine the spatio-

354 temporal variability patterns of R_s, we run Structural Equation Models (SEMs). SEMs analyses

355 allowed to test for the direct and indirect effects of all our measured in the field variables (i.e.,

356 microclimatic variables, forest structural and soil variables, and the micro-topography of the

357 terrain) on seasonal (i.e., spring, summer, autumn, and winter) R_s. SEMs analyses were carried

358 out using the "psem" function available from the "piecewiseSEM" R package (Lefcheck, 2016).

359 To harmonize the results of the SEMs with those obtained from the multiple regression

360 functions analyses, R_s was logarithmically transformed prior to analyses. Separated SEMs were

361 built for each of the four seasons (i.e., spring, summer, autumn, and winter). All SEMs were

362 designed based on hypotheses supported on simple univariate correlations between the different

363 microclimatic (i.e., soil temperature, T_s; soil water content, SWC), micro-topography of the

364 terrain (i.e., slope), soil (i.e., soil organic carbon content, SOC; and litter), and forest structural

365 (i.e., basal area, BA; number of trees, N_{trees}; diameter at breast height, DBH; mean distance,

366 MeanD; % of grass; and % of seedlings) variables (i.e., predictor variables). Furthermore, their

367 potential complex causal-effect relationships, that might determine the spatio-temporal

368 variability of R_s, were also considered. To test the goodness of fit of the SEMs, the Fisher's C

369 statistic was calculated. The Fisher's C statistic follows a chi-squared distribution and tests if

17

370   the model fits the data (p > 0.05) or not (p < 0.05). Several SEMs were run, the selection of the

371   best one being based on the AIC (Akaike Information Criteria) (Lefcheck, 2016).

372   All statistical analyses were carried out in R (v. 4.0.0, R Core Team, 2020). Statistical

373   relationships were considered significant at p < 0.05.

374

375   **3. Results**

376

377   *3.1.   The spatial variability of the forest structural and soil variables around the 81*

378   *soil respiration (R_s) measurement points*

379

380   We found a relatively low spatial variability (i.e., expressed here as relative variability, RV;

381   Table 1) for forest structural variables such as DBH (RV = 0.1) and MeanD (RV = 0.1) (Table

382   1, Figure S1). Similar results were obtained also for soil variables such as SOC (RV = 0.1) and

383   litter (RV = 0.1) (Table 1, Figure S1). On the other hand, the spatial variability of the understory

384   vegetation (i.e., % of grass and % of seedlings) showed the highest values and was higher

385   relative to the spatial variability of the overstorey vegetation (i.e., BA and N_{trees}) (Table 1,

386   Figure S1). High spatial variability values were found also for the slope (RV = 0.3) (Table 1,

387   Figure S1).

388

Statistics	BA (m^2 ha^{-1})	SOC (t ha^{-1})	Litter (cm)	Slope (%)	N_{trees} (N ha^{-1})	DBH (cm)	MeanD (m)	Grass (%)	Seedlings (%)
M	47.3	44.3	3.3	12.2	443	32.8	3.5	57.5	9.1
SD	16.9	12.9	0.7	8.3	200	6.3	0.8	31.1	8.6
RV	0.2	0.1	0.1	0.3	0.2	0.1	0.1	0.4	0.3

18

389   **Table 1.** Mean (M), standard deviation (SD), and relative variability (RV; following Lewontin

390   1966 and Webster 2001) values of forest structural, soil, and the micro-topography of the terrain

391   variables. *Where*, **BA**, basal area of the European beech trees surrounding the 81 measurement

392   points; **SOC**, soil organic carbon content; **Litter**, thickness of the litter layer; **Slope**, micro-

393   topography of the terrain within the study stand; N_{trees}, the count of all the surrounding

394   European beech trees around each of the 81 measurement points; **DBH**, average diameter at

395   breast height (i.e., > 6 cm) of the European beech trees surrounding the 81 measurement points;

396   **MeanD**, mean distance from the European beech trees to the 81 measurement points; **Grass**,

397   percentage of the soil surface covered by grass; **Seedlings**, percentage of the soil surface

398   covered by tree seedlings.

399

400   *3.2.*   *Soil respiration (R_s) sampling effort needed per season*

401

402   The calculation of the minimum number of measurements needed to obtain robust estimates of

403   R_s for each season (i.e., spring, summer, autumn, and winter) showed how sensitive *equation 1*

404   was to both the error limit (i.e., 10%, 20%, and 30%) and the confidence interval (90%, 95%,

405   and 99%) (Table S1). Accordinly, the calculated sampling effort varied within and among

406   seasons depending on the error limit and the confidence interval. Specifically, the sampling

407   effort varied more strongly within seasons than among them (Table S1). As for the sampling

408   effort needed from one season to another to obtain robust estimates of R_s, differences were not

409   so strong especially between summer, autumn, and winter (Table S1). Spring was the season

410   when less minimum R_s measurements seem to be needed to obtain robust estimates of R_s (Table

411   S1) no matter the confidence level and the error limit (Table S1). On the other hand, winter was

412   found to be the season when more sampling effort seems to be needed to obtain robust estimates

413   of R_s no matter the confidence level and the error limit (Table S1). The sampling effort for the

414   summer season seems to be quite close to the winter one, while the sampling effort for the

415   autumn season was found to be slightly lower (i.e., in between the spring and summer), no

416   matter the confidence level and the error limit (Table S1).

417

418   *3.3.   Seasonal and spatial variability of soil respiration (R_s), soil temperature (T_s),*

419   *and soil water content (SWC)*

420

421   As expected, both microclimatic variables (i.e., T_s and SWC) experienced very different

422   seasonal patterns during the study period (Table 2, Figure 2). On one hand, T_s experienced large

423   seasonal changes, peaking during summer and reaching its minimums during winter (Table 2,

424   Figure 2a). On the other hand, values of SWC experienced less seasonality, reaching its

425   minimums during summer, but being very stable and similar for the rest of the year (Table 2,

426   Figure 2b). Seasonality of R_s followed a pattern similar to that observed for T_s, peaking during

427   both spring and summer, and reaching its minimums during winter (Table 2, Figure 2c).

428

429   The spatial variability of the microclimatic variables was also markedly different (Table 2,

430   Figure 3). Specifically, the spatial variability of T_s was generally smaller (RV values ranging

431   from 0.01 to 0.10), within the range of 3.1 to 5.3 ºC of amplitude (Table 2, Figure 3A, D, G, J),

432   than the spatial variability of SWC (RV values ranging from 0.10 to 0.14), within the range of

433   31.9 to 54.6 % vol. of amplitude (Table 2, Figure 3B, E, H, K). R_s was the variable with the

434   highest spatial variability (RV values ranging from 0.13 to 0.17), within the range of 2.5 to 11.9

435    $\mu mol\ CO_2\ m^{-2}\ s^{-1}$ of amplitude (Table 2, Figure 3C, F, I, L) and coefficients of variation above

436   30% (Table 2). As concerning the standard deviation of the mean values, both T_s and SWC

437   showed seasonal changes, summer being the season that showed the lowest values (Table 2).

438   Standard deviation values for R_s also showed seasonal changes, being higher in spring and

439 summer and smaller in winter (Table 2), a pattern that followed the increase of the R_s rates

440 (Figure 2).

441

Period	T_s (°C)				SWC (% vol.)				R_s ($\mu mol\ CO_2\ m^{-2}\ s^{-1}$)				
	M	SD	RV	A	M	SD	RV	A	M	SD	RV	CV	A
Spring	14.4	0.9	0.03	4.6	33.0	10.2	0.14	54.6	6.3	2.0	0.13	31.1	8.7
Summer	17.4	0.6	0.01	3.1	24.9	6.6	0.12	31.9	6.4	2.4	0.17	37.6	11.9
Autumn	7.5	0.7	0.04	3.9	29.6	8.1	0.11	42.7	2.8	1.0	0.15	34.9	4.8
Winter	3.8	0.9	0.10	5.3	33.9	8.0	0.10	41.9	1.3	0.5	0.16	36.4	2.5
Annual	10.8	5.5	0.27	17.7	30.4	9.0	0.13	54.6	4.2	2.7	0.33	65.1	13.6

442 **Table 2.** Mean (M), standard deviation (SD), relative variability (RV; following Lewontin 1966

443 and Webster 2001), Coefficient of Variation (CV; only for the R_s variable) expressed as a

444 percentage, and absolute amplitude (A; defined as the difference between maximum and

445 minimum values) values of soil microclimate (i.e., T_s, soil temperature; and SWC, soil water

446 content) and soil respiration (R_s) measurements. The above mentioned statistics have been

447 calculated both at the seasonal level (i.e., spring, summer, autumn, and winter) and over the

448 four seasons combined (i.e., annual).

449

450 *3.4. The spatio-temporal variability of soil respiration (Rs)*

451

452 The model that best explained the microclimatic controls over the spatio-temporal variability

453 of R_s was the model that considered unimodal responses of R_s to T_s and a negative linear

454 response of R_s to SWC (i.e., equation 7) (Table S2, Figure 4). Specifically, the unimodal effect

455 of T_s on R_s translated into a seasonal sensitivity of R_s to T_s: i.e., R_s response to T_s was stronger

456 at lower T_s values (i.e., corresponding to autumn and winter seasons) than at higher T_s values

21

457   (i.e., corresponding to spring and summer seasons) (Figure 4a) when R_s reached its peak (Table

458   2) and its response to the seasonal changes of T_s was low. The overall effect of SWC over the

459   spatio-temporal variability of R_s was negative, this response being evidenced by the negative

460   slope of this relationship (Figure 4b). This negative effect was further on highlighted by the

461   overall relationship that was found between SWC and R_s at the spatial scale (i.e., results of the

462   SEM analyses), where higher values of SWC were generally associated with low R_s rates (see

463   Figures 4b and 5). Hence, the SWC effect on R_s was mainly driven by the spatially net negative

464   effect of SWC on R_s.

465

466   Both multiple regression functions and SEMs agreed that the microclimatic variables (T_s and

467   SWC; Figures 4 and 5) were, overall, the most important factors controlling the variability of

468   R_s in our 4.0 ha study stand. Nevertheless, SEMs further showed how the architecture of the

469   potential causal-effect relationships controlling R_s's spatial variability increased in complexity

470   (Figure 5) during spring and summer, when the spatial variability of R_s was maximal (see SD

471   and A in Table 2 and Figure 2C). Specifically, SEMs highlighted how during the summer

472   season, when the spatial variability of R_s was the highest (Table 2), the number of variables

473   ultimately involved in controlling the spatio-temporal variability of R_s were also high compared

474   to, e.g. winter or autumn (Figure 5). Also, the predictive capacity of the spatio-temporal

475   variability of R_s varied seasonally (Table 3), the coefficient of determination (R^2) ranging from

476   0.10 in winter to 0.29 in autumn. SEMs showed how both the forest structural (N_{trees}, MeanD,

477   and % of grass cover) and the micro-topography of the terrain (i.e., slope) variables may

478   strongly influence, directly and indirectly the spatio-temporal variability of R_s (Figure 5).

479   Specifically, in spring and summer, the % of grass cover was negatively associated with T_s and

480   SWC, which on their turn exerted a further positive and negative, respectively, influence on the

481   spatio-temporal variability of R_s (Figure 5). N_{trees} instead, always showed a direct and positive

482   effect on the spatio-temporal variability of R_s during the coldest seasons (i.e., autumn and

483   winter; Figure 5). The slope (i.e., the micro-topography of the terrain within the study stand)

484   was negatively related with MeanD in spring and summer, this relationship being especially

485   important during summer when MeanD exerted some control (i.e., positive relationship) over

486   R_s (Figure 5).

Season	Response	Predictor	Estimate	SE	df	p-value	SRW	Response	R^2	n	Fisher's C	df	p-value
Spring	R_s	T_s	0.0583	0.0154	78	0.0003	0.39	R_s	0.17	81	10.193	10	0.424
	R_s	Slope	-0.0031	0.0017	78	0.0672	-0.19	MeanD	0.05				
	MeanD	Slope	-0.0213	0.0103	79	0.0413	-0.23	T_s	0.07				
	T_s	Grass	-0.0076	0.0031	79	0.0170	-0.26						
Summer	R_s	SWC	-0.0086	0.0028	76	0.0030	-0.32	R_s	0.24	80	12.3	12	0.422
	R_s	T_s	-0.0836	0.0320	76	0.0109	-0.27	SWC	0.11				
	R_s	MeanD	0.0471	0.0227	76	0.0412	0.22	MeanD	0.05				
	SWC	Slope	-0.1890	0.0829	77	0.0253	-0.25						
	SWC	Grass	-0.0571	0.0226	77	0.0134	-0.28						
	MeanD	Slope	-0.0213	0.0103	79	0.0413	-0.23						
Autumn	R_s	T_s	0.0504	0.0233	77	0.0331	0.22	R_s	0.29	81	1.581	2	0.454
	R_s	SWC	-0.0076	0.0018	77	0.0001	-0.40	T_s	0.07				
	R_s	N_{trees}	0.0002	0.0001	77	0.0486	0.20						
	T_s	N_{trees}	0.0008	0.0004	79	0.0190	0.26						
Winter	R_s	N_{trees}	0.0003	0.0001	79	0.0045	0.31	R_s	0.10	81	0	0	1

487

24

488 **Table 3.** Statistics of the Structural Equation Models (SEMs) analyses showing causal-effect relationships that determine the spatio-temporal

489 variability of soil respiration (R_s). Only significant ($p < 0.05$) and marginally significant ($p < 0.1$) causal relationships are given. *Where*, T_s, soil

490 temperature; **SWC**, soil water content; **Slope**, micro-topography of the terrain within the study stand; N_{trees}, the count of all surrounding European

491 beech trees around each of the 81 measurement points; **MeanD**, mean distance from the European beech trees to the 81 measurement points; **Grass**,

492 percentage of the soil surface covered by grass; **SE**, standard error; **df**, degrees of freedom; **SRW**, Standardized Regression Weights; R^2, the

493 coefficient of determination; **n**, sampling size; **Fisher's C statistic**, follows a chi-squared distribution and tests if the model fits the data ($p > 0.05$)

494 or not ($p < 0.05$). The right hand part of the table shows the statistics of the best models representing the spatio-temporal variability of R_s during

495 each of the four different seasons (i.e., spring, summer, autumn, and winter).

496

497   **4. Discussion**

498

499   We here report high soil respiration (R_s) coefficient of variation values (i.e., CV, ranging from

500   31.1 in spring to 37.6 in summer; see Table 2) in an even-aged European beech study stand

501   located in the central-southern part of Romania (Mihaesti, Arges county). These values are

502   higher or comparable to other CV values mentioned in previous studies (e.g., Barba et al., 2013;

503   Epron et al., 2004*b*; Kosugi et al., 2007; Ngao et al., 2012; Shi et al., 2016; Stoyan et al., 2000),

504   although caution should be taken when comparing CV values among studies as they might also

505   vary depending on the considered spatial scales (e.g., Darenova & Čater, 2020; Ngao et al.,

506   2012). Nevertheless, independent of this consideration, the high CV values we obtained here

507   refute our first hypotheses (H1). In fact, the magnitude of the spatial variability of R_s during the

508   warmest seasons (i.e., spring and summer) was comparable to the overall annual variability of

509   R_s (see SD and A values in Table 2), which reinforces the idea of the large, though generally

510   neglected, impact of R_s's spatial variability on estimates of soil CO_2 effluxes, even in

511   homogenous ecosystems such as the European beech even-aged study stand that we considered

512   here. The calculated large sampling effort needed to obtain robust estimates of R_s for any given

513   season (being even larger in winter, see Table S1) further highlights the importance of the

514   spatial variability of R_s as a potential source of uncertainty on local and global CO_2 estimates

515   and that should be taken into account. This is of upmost importance especially now, when the

516   number of studies dedicated to scale up CO_2 observations from local to global levels is growing.

517   Accordingly, our study suggests that obtaining robust estimates of R_s at the local level may

518   require of more intense spatial sampling efforts, than those generally carried out for logistical

519   reasons, in order to address and diagnose uncertainties on CO_2 estimates at the global level

520   (e.g., Jian et al., 2018; Warner et al., 2019).

521

522   The large spatio-temporal variability of R_s was strongly and directly determined by soil

523   microclimatic conditions (T_s and SWC; Figures 4 and 5). Nevertheless, as hypothesized (H2),

524   less considered variables such as the forest structural ones (i.e., grass, MeanD, N_{trees}) or the

525   micro-topography of the terrain (i.e., slope), proved to have a determinant, direct or indirect,

526   effect on the observed spatio-temporal variability of R_s. In the case of the slope and the grass

527   cover variables, they both showed further tight relationships with soil microclimatic conditions

528   (i.e., T_s and SWC). These relationships were found to be significant in spring and summer

529   (Figure 5), the two seasons when R_s values peaked (Table 2). Specifically, grass cover

530   modulated the T_s variable in spring, with an indirect effect over R_s. In summer instead, when

531   SWC usually registers low values and the competition for water and nutrients between the

532   heterotrophic communities and the vegetation is high (Villegas et al., 2010), grass cover

533   modulated the SWC availability, with an indirect effect over R_s. Our results highlight thus the

534   importance of seldom considered variables, such as the micro-topography of the terrain (e.g.,

535   Arias-Navarro et al., 2017) and the vegetation (e.g., Søe & Buchmann, 2005), in R_s studies, as

536   they may actually substantially impact, either directly or indirectly, the spatio-temporal

537   variability of R_s. Instead, in our European beech even-aged study stand, we found no significant

538   effects of variables generally well associated with the spatial variability of R_s, such as the litter

539   (e.g., Epron et al., 2004*b*; Katayama et al., 2009; Saiz et al., 2006) or the soil organic carbon

540   content (e.g., Søe & Buchmann, 2005). Although the fact that litter thickness was only

541   measured once (i.e., during the 2016 summer; cf. 2.3. section), and thus may have generated a

542   certain source of noise in our models (since the litter generally accumulates in autumn in

543   deciduous-dominated forests), we assumed that our summer measurements contain very

544   valuable information on the long-term spatial patterns of litter accumulation on the soil, and

545   therefore, valuable information on where litter can have a greater impact on the spatial

546   variability of soil processes in the long term. We are further aware of the limitations of our

547   study, since other variables, such as soil compaction (Schwen et al., 2015) or the spatial

548   distribution of the root biomass (Søe & Buchmann, 2005), that have not been measured, may

549   have also helped to explain the observed spatial patterns of R_s. However, we expect that effects

550   of the spatial variability of soil compaction on, e.g. water infiltration or CO_2 diffusivity (e.g.,

551   Schwen et al., 2015), will not be as high as in more intensively used stands since our study

552   stand has not undergone any forestry intervention during the last 85 years and has no livestock

553   load (according to the Mihaesti Forest Management Plan). On the other hand, and given the

554   logistical inability to obtain estimates of the spatial distribution of root biomass, our exhaustive

555   characterization of the distribution of trees and understorey (e.g., grass and seedlings) around

556   the 81 measurement points emerged as a good proxy highly associated with the distribution of

557   roots, assuming that proximity to vegetation is closely associated with root density in the soil

558   (Søe & Buchmann, 2005).

559

560   Our results further emphasized the importance of understanding the temporal (i.e., seasonal)

561   changes in the magnitude and controls of spatial variability of R_s. This variability could be

562   especially important in temperate areas where microclimatic conditions (i.e., T_s and SWC), soil

563   CO_2 effluxes, and vegetation activity may vary dramatically throughout the year (e.g., Curiel

564   Yuste et al., 2005). Indeed, and also as hypothesized (H3), our results indicated that, along with

565   the observed seasonal variability in the magnitude of R_s, the variables that control the spatial

566   variability of R_s were also subjected to strong seasonality. The architecture of the causal-effect

567   relationships controlling R_s's spatial variability varied between the four seasons and showed an

568   increased complexity during spring and summer, while in autumn and especially in winter these

569   relationships were much simpler (Figure 5). In line with these findings, spring and summer

570   were also the seasons when the highest R_s values were registered, as expected for temperate

571   ecosystems (e.g., Knohl et al., 2008; Saiz et al., 2006; Shi et al., 2016; Søe & Buchmann, 2005).

28

572 These high R_s values coincided thus with the warmest temperatures of the year, with the peak

573 in plant and soil biological activity, and with the highest variability of R_s in absolute terms.

574 These results are of upmost importance as they highlight the fact that in order to obtain robust

575 estimates of R_s-CO_2 derived emissions and to have a deeper understanding on the R_s variability,

576 both spatial and temporal R_s controlling processes need to be taken into account.

577

578 Based on our results, we postulate that in this even-aged European beech study stand, the

579 observed spatio-temporal changes and controls of the R_s respond to a seasonal shift that goes

580 from temperature-controlled (i.e., winter and autumn) to water-controlled (i.e., spring and

581 summer) processes. Figure 6 shows a conceptual framework, based on our results, that

582 illustrates this shift in time. During cold periods, when the seasonal variability of R_s was, as

583 expected in a temperature forest (e.g., Curiel Yuste et al. 2003), strongly limited by T_s (Figure

584 4a), the spatial variability in R_s followed the low spatial variability of T_s (represented as

585 standard deviation of the mean R_s or T_s in Figure 6), resulting in low spatial variability of R_s

586 (Table 2, Figure 6). Most factors had insignificant effects over the spatial variability of R_s

587 during the winter season, when only N_{trees} (i.e., the number of European beech trees surrounding

588 the 81 measurement points) showed a positive relationship with R_s (Figure 5). These results

589 might be related with a larger autotrophic respiration contribution to R_s during winter when

590 European beech trees are able to maintain part of their fine root biomass alive (e.g., Büttner and

591 Leuschner, 1994; Zwetsloot et al., 2019). A similar result was found for the autumn season,

592 when N_{trees} also showed a positive relationship with R_s (Figure 5). During warm periods (i.e.,

593 summer), when the soil metabolic activity is at its peak (reflected in higher rates of R_s; Table

594 2, Figure 2), the increase in temperature and vegetation activity increases the demand for SWC

595 (evapotranspiration), which then becomes a limiting factor for R_s. Although our SWC

596 measurements were too deep (i.e., 20 cm soil depth) to capture this increasing water control

29

597   (i.e., our model could not capture a positive effect of SWC on R_s; see Figure 4b), this seasonal

598   water limitation of R_s was evidenced by the low sensitivity to temperature that R_s experienced

599   during the warmer periods (Figure 4a), which is the shape typically observed when R_s responds

600   to a shift that goes from temperature-controlled to water-controlled processes (e.g., Curiel-

601   Yuste et al., 2003, 2005; Davidson & Janssens, 2006). This shift towards R_s's spatial variability

602   being water-controlled resulted in an increase in R_s variability, which subsequently become

603   more spatially variable than temperature (reflected in increased standard deviation values of R_s

604   with respect to T_s; see Figure 6). The shift towards a water-limited R_s system that generated

605   spatial variability of R_s (Figure 6) also increased the complexity of R_s controls (Figures 5 and

606   6). This is because the increase in vegetation activity triggered a higher competition for water,

607   as evidenced by, e.g. the strong negative influence of tree proximity (i.e., positive effect of

608   MeanD in summer on R_s; Figure 5) or the strong negative effect of the grass cover over SWC

609   during summer (Figure 5). Hence, the evaporative demand of the vegetation (i.e., MeanD and

610   grass cover) exerted direct and indirect controls over the spatial variability of R_s during dry,

611   warm, and phenologically active periods (i.e., spring and summer), contributing to an increase

612   in the spatial variability of R_s. The slope (i.e., the micro-topography of the terrain) was another

613   variable that contributed, directly and indirectly, to the increase in the spatial variability of R_s

614   during warmer periods characterized by higher water demand (Figure 5). Slope may have large

615   impacts over water availability and water balances by creating spatial variability in e.g. the

616   incidence of solar radiation at the floor level and water run-off (Berryman et al., 2015; Riveros-

617   Iregui et al., 2012), with further consequences on soil CO_2 effluxes, even across short distances

618   (Arias-Navarro et al., 2017). It is likely that, at our study stand, the spatial distribution of the

619   slopes captured the spatial variability of SWC during drier periods (i.e., summer) better than

620   our own SWC measurements taken at 20 cm depth. This is because during periods of high water

621   demand (i.e., summer), SWC decreases very fast in the uppermost layer of the soil, where most

622 of both autotrophic and heterotrophic activities concentrate (Curiel Yuste et al., 2003, 2005),

623 whereas at 20 cm depth SWC remains above the volumetric content thresholds at which SWC

624 limits Rs, as stated by the fact that no positive relationship was found between SWC and R_s

625 (Figures 4b and 5).

626

627 **5. Conclusions**

628

629 We here highlight the fact that the spatial variability of R_s proves to be high even in a relatively

630 homogenous even-aged European beech study stand of 4.0 ha. Accordingly, our estimates

631 regarding the sampling effort needed to obtain robust estimates of R_s further suggest that most

632 studies to date might have probably underestimated the sampling effort needed to obtain

633 accurate spatial estimates of R_s throughout the year. Our study further shows that the spatial

634 variability of R_s, varied significantly throughout the year, peaking in spring and summer and

635 being low in winter, coinciding thus with the seasonal variability in the absolute magnitude of

636 R_s. We here postulate that in this European beech-dominated even-aged study stand, the

637 observed large seasonal changes in the magnitude and controls of the spatial variability of R_s

638 respond to a seasonal shift that goes from temperature-controlled (i.e., winter and autumn) to

639 water-controlled (i.e., spring and summer) processes. This is because when temperatures and

640 water demands are high, the evaporative demand of both the overstorey but also the understorey

641 vegetation, as well as the micro-topography of the terrain (i.e., slope), generate spatial

642 complexity in soil R_s. During winter, temperature limits processes and prevents most other

643 factors from spatially influencing R_s. In conclusion, obtaining robust, accurate estimates of R_s-

644 derived CO_2 effluxes, may profit from: (1) a deeper understanding of how the spatial patterns

645 of R_s varies across seasons, e.g., understanding when processes shift from being controlled by

646 temperature (i.e., winter and autumn) to being controlled by water (i.e., spring and summer);

31

647 and (2) a deeper understanding on how, when, and where, factors such as the micro-topography

648 of the terrain or the plant-plant and the plant-soil competition for water may contribute to this

649 spatial variability of R_s. In line with our findings, it would be interesting to test in future at

650 which extent this observed trends apply to other types of ecosystems or if they may also be

651 extrapolated to latitudinal and/or altitudinal gradients, i.e., whether R_s's spatial complexity may

652 increase considering gradients that go from temperature-limited (e.g., temperate) to water-

653 limited (e.g., arid and semi-arid) systems, or from topographically simple (e.g., valleys) to

654 topographically more complex (e.g., mountains) systems.

655

656 **Acknowledgements**

657

667

References

Allaire, S.E., Lange, S.F., Lafond, J.A., Pelletier, B., Cambouris, A.N. & Dutilleul P. (2012). Multiscale spatial variability of CO_2 emissions and correlations with physico-chemical soil properties. *Geoderma*, 170, 251-260. https://doi.org/10.1016/j.geoderma.2011.11.019

Arias-Navarro, C., Díaz-Pinés, E., Klatt, S., Brandt, P., Rufino, M.C., Butterbach-Bahl, K. & Verchot, L.V. (2017). Spatial variability of soil N_2O and CO_2 fluxes in different topographic positions in a tropical montane forest in Kenya. *Journal of Geophysical Research: Biogeosciences*, 122, 514-527. https://doi.org/10.1002/2016JG003667

Bahn, M., Reichstein, M., Davidson, E.A., Grünzweig, J., Jung, M., Carbone, M.S., Epron, D., Misson, L., Nouvellon, Y., Roupsard, O., Savage, K., Trumbore, S.E., Gimeno. C., Curiel Yuste, J., Tang, J., Vargas, R. & Janssens, I.A. (2009). Soil respiration at mean annual temperature predicts annual total across vegetation types and biomes. *Biogeosciences*, 7, 2147-2157. 10.5194/bg-7-2147-2010

Barba, J., Cueva, A., Bahn, M., Barron-Gafford, G.A., Bond-Lamberty, B., Hanson, P.J., Jaimes, A., Kulmala, L., Pumpanen, J., Scott, R.L., Wohlfahrt, G. & Vargas, R. (2018). Comparing ecosystem and soil respiration: Review and key challenges of tower-based and soil measurements. *Agricultural and Forest Meteorology*, 249, 434-443. https://doi.org/10.1016/j.agrformet.2017.10.028

Barba, J., Curiel Yuste, J., Martínez-Vilalta, J. & Lloret, F. (2013). Drought-induced tree species replacement is reflected in the spatial variability of soil respiration in a mixed

692   Mediterranean   forest. *Forest   Ecology   and   Management*, *306*,   79-87.

693   https://doi.org/10.1016/j.foreco.2013.06.025

694

695   Berryman, E.M., Barnard, H.R., Adams, H.R., Burns, M.A., Gallo, E. & Brooks, P.D. (2015).

696   Complex terrain alters temperature and moisture limitations of forest soil respiration across a

697   semiarid to subalpine gradient. *Journal of Geophysical Research: Biogeosciences*, 120, 707-

698   723. https://doi.org/10.1002/2014JG002802

699

700   Birch, H.F. (1958). The effect of soil drying on humus decomposition and nitrogen availability.

701   *Plant and Soil*, 10, 9-31. https://doi.org/10.1007/BF01343734

702

703   Bond-Lamberty, B. & Thomson, A. (2010). Temperature-associated increases in the global soil

704   respiration record. *Nature*, 464, 579-582. https://doi.org/10.1038/nature08930

705

706   Brito, L.F., Marques Júnior, J., Pereira, G.T. & La Scala Junior, N. (2010). Spatial variability

707   of soil CO_2 emission in different topographic positions. *Bragantia*, 69, 19-27.

708   http://dx.doi.org/10.1590/S0006-87052010000500004

709

710   Büttner, V. & Leuschner, C. (1994). Spatial and temporal patterns of fine root abundance in a

711   mixed oak-beech forest. *Forest Ecology and Management*, 70, 11–21.

712   https://doi.org/10.1016/0378-1127(94)90071-X

713

714   Chen, S., Zou, J., Hu, Z., Chen, H. & Lu, Y. (2014). Global annual soil respiration in relation

715   to climate, soil properties and vegetation characteristics: Summary of available

716   data. *Agricultural   and   Forest   Meteorology*, 198-199,   335-346.

717   https://doi.org/10.1016/j.agrformet.2014.08.020

718

719   Curiel Yuste J., Janssens, I.A., Carrara, A., Meiresonne, L. & Ceulemans, R. (2003). Interactive

720   effects of temperature and precipitation on soil respiration in a temperate maritime pine forest.

721   *Tree Physiology*, 23, 1263-1270. https://doi.org/10.1093/treephys/23.18.1263

722

723   Curiel Yuste, J., Nagy, M., Janssens, I.A., Carrara, A. & Ceulemans, R. (2005). Soil respiration

724   in a mixed temperate forest and its contribution to total ecosystem respiration. *Tree Physiology*,

725   25, 609-619. https://doi.org/10.1093/treephys/25.5.609

726

727   Curiel Yuste, J., Flores-Rentería, D., García-Angulo, D., Hereş, A.-M., Bragă, C., Petritan, A.-

728   M. & Petritan, I.C. (2019). Cascading effects associated with climate-change-induced conifer

729   mortality in mountain temperate forests result in hot-spots of soil CO_2 emissions. *Soil Biology*

730   *& Biochemistry*, 133, 50-59. https://doi.org/10.1016/j.soilbio.2019.02.017

731

732   Darenova, E. & Čater, M. (2020). Effect of spatial scale and harvest on heterogeneity of forest

733   floor CO_2 efflux in a sessile oak forest. *Catena*, 188, 104455,

734   https://doi.org/10.1016/j.catena.2020.104455

735

736   Davidson, E.A., Belk, E. & Boone, R.D. (1998). Soil water content and temperature as

737   independent or confounded factors controlling soil respiration in a temperate mixed hardwood

738   forest. *Global Change Biology*, 4, 217-227. https://doi.org/10.1046/j.1365-2486.1998.00128.x

739

740   Davidson, E.A., Verchot, L.V., Cattânio, J.H., Ackerman, I.L. & Carvalho, J.E.M. (2000).

741   Effects of soil water content on soil respiration in forests and cattle pastures of eastern

742   Amazonia. *Biogeochemistry*, 48, 53-69. https://doi.org/10.1023/A:1006204113917

743

744   Davidson, E.A., Savage, K., Verchot, L.V. & Navarro, R. (2002). Minimizing artifacts and

745   biases in chamber-based measurements of soil respiration. *Agricultural and Forest*

746   *Meteorology*, 113, 21-37. https://doi.org/10.1016/S0168-1923(02)00100-4

747

748   Davidson, E.A. & Janssens, I.A. (2006). Temperature sensitivity of soil carbon decomposition

749   and feedbacks to climate change. *Nature*, 440, 165-173. https://doi.org/10.1038/nature04514

750

751   de Gruijter, J., Brus, D.J., Bierkens, M.F.P. & Knotters, M. (2006). Sampling for Natural

752   Resource Monitoring. Springer-Verlag Berlin Heidelberg. 10.1007/3-540-33161-1

753

754   Epron, D., Ngao, J. & Granier, A. (2004*a*). Interannual variation of soil respiration in a beech

755   forest ecosystem over a six-year study. *Annals of Forest Science*, 61, 499-505.

756   https://doi.org/10.1051/forest:2004044

757

758   Epron, D., Nouvellon, Y., Roupsard, O., Mouvondy, W., Mabiala, A., Saint-André, L., Joffre,

759   R., Jourdan, C., Bonnefond, J.-M., Berbigier, P. & Hamel, O. (2004*b*). Spatial and temporal

760   variations of soil respiration in a *Eucalyptus* plantation in Congo. *Forest Ecology and*

761   *Management*, 202, 149-160. https://doi.org/10.1016/j.foreco.2004.07.019

762

763   Florea, N. & Munteanu, I. (2012). Sistemul Roman de Taxonomie a Solurilor – SRTS (in

764   Romanian). Editura Sitech, Craiova, Romania.

765

766 Hanson, P.J., Wullschleger, S.D., Bohlman, S.A. & Todd, D.E. (1993). Seasonal and

767 topographic patterns of forest floor CO_2 efflux from an upland oak forest. *Tree Physiology*, 13,

768 1-15. https://doi.org/10.1093/treephys/13.1.1

769

770 Harris, I., Osborn, T.J., Jones, P., Lister, D., 2020. Version 4 of the CRU TS monthly high-

771 resolution gridded multivariate climate dataset. Scientific Data 7, 109.

772 https://doi.org/10.1038/s41597-020-0453-3.

773

774 Herbst, M., Prolingheuer, N., Graf, A., Huisman, J.A., Weihermüller, L. & Vanderborght, J.

775 (2009). Characterization and understanding of bare soil respiration spatial variability at plot

776 scale. *Vadose Zone Journal*, 8, 762-771. https://doi.org/10.2136/vzj2008.0068

777

778 Janssens, I.A., Lankreijer, H., Matteucci, G., Kowalski, A.S., Buchmann, N., Epron, D.,

779 Pilegaard, K., Kutsch, W., Longdoz, B., Grünwald, T., Montagnani, L., Dore, S., Rebmann, C.,

780 Moors, E.J., Grelle, A., Rannik, Ü., Morgenstern, K., Oltchev, S., Clement, R., Guðmundsson,

781 J., Minerbi, S., Berbigier, P., Ibrom, A., Moncrieff, J., Aubinet, M., Bernhofer, C., Jensen, N.O.,

782 Vesala, T., Granier, A., Schulze, E.D., Lindroth, A., Dolman, A.J., Jarvis, P.G., Ceulemans, R.

783 & Valentini, R. (2001). Productivity overshadows temperature in determining soil and

784 ecosystem respiration across European forests. *Global Change Biology*, 7, 269-278.

785 https://doi.org/10.1046/j.1365-2486.2001.00412.x

786

787 Jian, J., Steele, M.K., Thomas, R.Q., Day, S.D. & Hodges, S.C. (2018). Constraining estimates

788 of global soil respiration by quantifying sources of variability. *Global Change Biology*, 24,

789 4143– 4159. https://doi.org/10.1111/gcb.14301

790

791   Katayama, A., Kume, T., Komatsu, H., Ohashi, M., Nakagawa, M., Yamashita, M., Otsuki, K.,

792   Suzuli, M. & Kumagai, T. O. (2009). Effect of forest structure on the spatial variation in soil

793   respiration in a Bornean tropical rainforest. *Agricultural and Forest Meteorology*, 149, 1666-

794   1673. https://doi.org/10.1016/j.agrformet.2009.05.007

795

796   Khomik, M., Arain, M.A. & McCaughey, J.H. (2006). Temporal and spatial variability of soil

797   respiration in a boreal mixedwood forest. *Agricultural and Forest Meteorology*, 140, 244-256.

798   https://doi.org/10.1016/j.agrformet.2006.08.006

799

800   Kosugi, Y., Mitani, T., Itoh, M., Noguchi, S., Tani, M., Matsuo, N., Takanashi, S., Ohkubo, S.

801   & Nik, A.R. (2007). Spatial and temporal variation in soil respiration in a Southeast Asian

802   tropical   rainforest. *Agricultural   and   Forest   Meteorology*, 147,   35-47.

803   https://doi.org/10.1016/j.agrformet.2007.06.005

804

805   Knohl, A., Søe, A.R.B., Kutsch, W.L., Göckede, M. & Buchmann, N. (2008). Representative

806   estimates of soil and ecosystem respiration in an old beech forest. *Plant and Soil*, 302, 189-202.

807   https://doi.org/10.1007/s11104-007-9467-2

808

809   Law, B.E., Kelliher, F.M., Baldocchi, D.D., Anthoni, P.M., Irvine, J., Moore, D. & Van Tuyl,

810   S. (2001). Spatial and temporal variation in respiration in a young ponderosa pine forest during

811   a   summer   drought. *Agricultural   and   Forest   Meteorology*, 110,   27-43.

812   https://doi.org/10.1016/S0168-1923(01)00279-9

813

814   Lefcheck, J.S. (2016). piecewiseSEM: Piecewise structural equation modelling in R for

815   ecology, evolution, and systematics. *Methods in Ecololgy Evolution*, 7, 573-579.

816   https://doi.org/10.1111/2041-210X.12512

817

818   Lewontin, R.C. (1966). On the Measurement of Relative Variability. *Systematic Biology*, 15,

819   141-142. https://doi.org/10.2307/sysbio/15.2.141

820

821   Maestre, F.T. & Cortina, J. (2003). Small-scale spatial variation in soil CO_2 efflux in a

822   Mediterranean   semiarid   steppe. *Applied   Soil   Ecology*, 23,   199-209.

823   https://doi.org/10.1016/S0929-1393(03)00050-7

824

825   Ngao, J., Epron, D., Delpierre, N., Bréda, N., Granier, A. & Longdoz, B. (2012). Spatial

826   variability of soil CO_2 efflux linked to soil parameters and ecosystem characteristics in a

827   temperate beech forest. *Agricultural and Forest Meteorology*, 154-155, 134-146.

828   https://doi.org/10.1016/j.agrformet.2011.11.003

829

830   Oishi, A.C., Palmroth, S., Butnor, J.R., Johnsen, K. & Oren, R. (2013). Spatial and temporal

831   variability of soil CO_2 efflux in three proximate temperate forest ecosystems. *Agricultural and*

832   *Forest Meteorology*, 171-172, 256-269. https://doi.org/10.1016/j.agrformet.2012.12.007

833

834   Poblador, S., Lupon, A., Sabaté, S. & Sabater, F. (2017). Soil water content drives

835   spatiotemporal patterns of CO_2 and N_2O emissions from a Mediterranean riparian forest

836   soil. *Biogeosciences*, 14, 4195-4208. https://doi.org/10.5194/bg-14-4195-2017

837

838 R Core Team (2020). R (v. 4.0.0, 2020): A language and environment for statistical computing.

839 R Foundation for Statistical Computing, Vienna, Austria. URL http://www.R-project.org/

840

841 Raich, J.W. & Schlesinger, W.H. (1992). The global carbon dioxide flux in soil respiration and

842 its relationship to vegetation and climate. *Tellus B: Chemical and Physical Meteorology*, 44,

843 81-99. https://doi.org/10.3402/tellusb.v44i2.15428

844

845 Raich, J.W. & Tufekcioglu, A. (2000). Vegetation and soil respiration: Correlation and controls.

846 *Biogeochemistry*, 48, 71-90. https://doi.org/10.1023/A:1006112000616

847

848 Rayment, M.B. & Jarvis, P.G. (2000). Temporal and spatial variation of soil CO_2 efflux in a

849 Canadian boreal forest. *Soil Biology & Biochemistry*, 32, 35-45. https://doi.org/10.1016/S0038-

850 0717(99)00110-8

851

852 Ribeiro Jr., P.J., Diggle, P.J., Schlather, M., Bivand, R. & Ripley, B. (2020). geoR: Analysis of

853 Geostatistical Data. R package version 1.8-1. https://CRAN.R-project.org/package=geoR

854

855 Riveros-Iregui, D.A., McGlynn, B.L., Emanuel, R.E. & Epstein, H.E. (2012). Complex terrain

856 leads to bidirectional responses of soil respiration to inter-annual water availability. *Global*

857 *Change Biology*, 18, 749-756. https://doi.org/10.1111/j.1365-2486.2011.02556.x

858

859 Rodeghiero, M. & Cescatti, A. (2008). Spatial variability and optimal sampling strategy of soil

860 respiration. *Forest   Ecology   and   Management*, 255,   106-112.

861 https://doi.org/10.1016/j.foreco.2007.08.025

862

863 Saiz, G., Green, C., Butterbach-Bahl, K., Kiese, R., Avitabile, V. & Farrell, E.P. (2006).

864 Seasonal and spatial variability of soil respiration in four Sitka spruce stands. *Plant and*

865 *Soil*, 287, 161-176. https://doi.org/10.1007/s11104-006-9052-0

866

867 Shi, B., Gao, W., Cai, H. & Jin, G. (2016). Spatial variation of soil respiration is linked to the

868 forest structure and soil parameters in an old-growth mixed broadleaved-Korean pine forest in

869 northeastern China. *Plant and Soil*, 400, 263-274. https://doi.org/10.1007/s11104-015-2730-z

870

871 Silvola, J., Alm, J., Ahlholm, U., Nykanen, H., & Martikainen, P.J. (1996). CO_2 fluxes from

872 peat in boreal mires under varying temperature and moisture conditions. *Journal of Ecology*,

873 219-228. https://www.jdoi.org./10.2307/2261357

874

875 Søe, A.R.B. & Buchmann, N. (2005). Spatial and temporal variations in soil respiration in

876 relation to stand structure and soil parameters in an unmanaged beech forest. *Tree*

877 *Physiology*, 25, 1427-1436. https://doi.org/10.1093/treephys/25.11.1427

878

879 Stoyan, H., De-Polli, H., Böhm, S., Robertson, G.P. & Paul, E.A. (2000). Spatial heterogeneity

880 of soil respiration and related properties at the plant scale. *Plant and Soil*, 222, 203-214.

881 https://doi.org/10.1023/A:1004757405147

882

883 Sánchez-Cañete, E.P., Oyonarte, C., Serrano-Ortiz, P., Curiel Yuste, J., Pérez-Priego, O.,

884 Domingo, F. & Kowalski, A.S. (2016). Winds induce CO_2 exchange with the atmosphere and

885 vadose zone transport in a karstic ecosystem. *Journal of Geophysical Research:*

886 *Biogeosciences*, 121, 2049-2063. https://doi.org/10.1002/2016JG003500

887

41

888   Schwen, A., Jeitler, E. & Böttcher, J. (2015). Spatial and temporal variability of soil gas

889   diffusivity, its scaling and relevance for soil respiration under different tillage. *Geoderma*, 259-

890   260, 323-336. https://doi.org/10.1016/j.geoderma.2015.04.020

891

892   Venables, W.N. & Ripley, B.D. (2002). Modern Applied Statistics with S, Fourth edition.

893   Springer, New York. ISBN 0-387-95457-0, http://www.stats.ox.ac.uk/pub/MASS4/

894

895   Vicca, S., Bahn, M., Estiarte, M., van Loon, E.E., Vargas, R., Alberti, G., Ambus, P., Arain, M.

896   A., Beier, C., Bentley, L. P., Borken, W., Buchmann, N., Collins, S.L., de Dato, G., Dukes, J.

897   S., Escolar, C., Fay, P., Guidolotti, G., Hanson, P. J., Kahmen, A., Kröel-Dulay, G., Ladreiter-

898   Knauss, T., Larsen, K. S., Lellei-Kovacs, E., Lebrija-Trejos, E., Maestre, F.T., Marhan, S.,

899   Marshall, M., Meir, P., Miao, Y., Muhr, J., Niklaus, P.A., Ogaya, R., Peñuelas, J., Poll, C.,

900   Rustad, L.E., Savage, K., Schindlbacher, A., Schmidt, I.K., Smith, A.R., Sotta, E.D., Suseela,

901   V., Tietema, A., van Gestel, N., van Straaten, O., Wan, S., Weber, U. & Janssens, I. A. (2014).

902   Can current moisture responses predict soil CO_2 efflux under altered precipitation regimes? A

903   synthesis   of   manipulation   experiments.   *Biogeosciences*,   11,   2991-3013.

904   https://doi.org/10.5194/bg-11-2991-2014

905

906   Villegas, J. C., D. D. Breshears, C. B. Zou, and P. D. Royer. (2010). Seasonally Pulsed

907   Heterogeneity in Microclimate: Phenology and Cover Effects along Deciduous Grassland–

908   Forest Continuum. *Vadose Zone Journal*, 9, 537-547. https://doi.org/10.2136/vzj2009.0032

909

910   Wang, W.J., Zu, Y.G., Wang, H.M., Hirano, T., Takagi, K., Sasa, K. & Koike, T. (2005). Effect

911   of collar insertion on soil respiration in a larch forest measured with a LI-6400 soil CO_2 flux

912   system. *Journal of Forest Research*, 10, 57-60. https://doi.org/10.1007/s10310-004-0102-2

913

914   Warner, D.L., Bond-Lamberty, B., Jian, J., Stell, E. & Vargas, R. (2019). Spatial predictions

915   and associated uncertainty of annual soil respiration at the global scale. *Global Biogeochemical*

916   *Cycles*, 33, 1733– 1745. https://doi.org/10.1029/2019GB006264

917

918   Webster, R. (2001). Statistics to support soil research and their presentation. *European*

919   *Journal of Soil Science*, 52, 331-340. https://doi.org/10.1046/j.1365-2389.2001.00383.x

920

921   Zuur, A.F., Ieno, E.N. & Elphick, C.S. (2010). A protocol for data exploration to avoid common

922   statistical problems. *Methods in Ecology and Evolution*, 1, 3-14. https://doi.org/10.1111/j.2041-

923   210X.2009.00001.x

924

925   Zwetsloot, M.J., Goebel. M., Paya, A., Grams, T.E.E. & Bauerle, T.L. (2019). Specific spatio-

926   temporal dynamics of absorptive fine roots in response to neighbor species identity in a mixed

927   beech–spruce forest. *Tree Physiology*, 39, 1867-1879. https://doi.org/10.1093/treephys/tpz086

928

929 **Figure captions:**

930 **Figure 1.** Map indicating the location of Romania within Europe and the location of the study

931 site in the central-southern part of Romania (i.e., Mihaesti, Arges county). The small panel

932 shows the sampling design: a 4.0 ha (i.e., 200 m x 200 m) even-aged European beech stand

933 divided into 25 m x 25 m squares. The scale that appears on the right size of the small panel

934 indicates the altitude (m a.s.l.) gradient within the study stand.

935 **Figure 2**. Seasonal (i.e., spring, summer, autumn, and winter) patterns of: a) soil temperature

936 (T_s); b) soil water content (SWC); and c) soil respiration (R_s).

937 **Figure 3**. Spatial prediction based on the fixed covariance parameters generated by performing

938 geostatistical analyses on the seasonal (i.e.., spring, summer, autumn, and winter) spatial

939 distribution of soil temperature (T_s), soil water content (SWC), and soil respiration (R_s).

940 **Figure 4**. Representation of the best model (Table S2) that explained the microclimatic controls

941 (soil temperature, T_s; and soil water content, SWC) over the spatio-temporal variability of soil

942 respiration (R_s): a) R_s response to T_s; and b) R_s response to SWC. Black opened dots represent

943 the row data, while red (i.e., R_s response to T_s model) and blue (i.e., R_s response to SWC model)

944 opened dots represent the fitted by the best model data. To ease the interpretation, the results of

945 the multiple regression functions, for which R_s was logarithmically transformed, were back-

946 transformed to the original scale.

947 **Figure 5**. Path diagrams showing the results of the Structural Equation Models (SEMs),

948 represented by seasons. Arrows indicate causal relationships: positive and negative effects are

949 indicated by solid and dashed arrows, respectively. Only the significant ($p < 0.05$) and

950 marginally significant ($p < 0.1$) relationships were represented (see Table 3). The number given

951 next to each arrow represents the Standardized Regression Weights (SRW) values given in

952 Table 3. Path diagrams are represented in a plot where the X-axis represents the seasons (i.e.,

953 spring, summer, autumn, and winter) and the Y-axis represents the mean values of the soil

44

954 respiration (R_s) flux for each season. *Where*, **Grass**, percentage of the soil surface covered by

955 grass; T_s, soil temperature; R_s, soil respiration; **Slope**, micro-topography of the terrain within

956 the study stand; **MeanD**, mean distance from the European beech trees to the 81 measurement

957 points; **SWC**, soil water content; N_{trees}, the count of all the surrounding European beech trees

958 around each of the 81 measurement points.

959 **Figure 6.** Conceptual framework illustrating how the observed spatio-temporal changes and

960 environmental controls of the soil respiration (R_s) respond to a seasonal shift that goes from

961 temperature-controlled (i.e., winter and autumn) to water-controlled (i.e., spring and summer)

962 processes. The X-axis represents the seasonal (i.e., winter, autumn, spring, and summer) soil

963 temperature (T_s) changes. The Y-axis represents the spatial variability of soil temperature (T_s)

964 and R_s represented as the standard deviation (SD) of the mean. The path diagrams, obtained

965 from the Structural Equation Models (SEMs; Figure 5), are also represented to show how the

966 complexity of the controls of R_s increases along with the spatial variability of R_s. In the upper

967 part of the figure, the shift that goes from temperature-controlled (i.e., winter and autumn) to

968 water-controlled (i.e., spring and summer) processes over the spatial variability of R_s, is

969 indicated. The small figure panel included within the conceptual framework is represented by

970 Figure 4*a*, with the red arrows indicating the seasonal temperature control of R_s (winter and

971 autumn) and the flattening of this control during warmer periods (spring and summer). *Where*,

972 N_{trees}, the count of all the surrounding European beech trees around each of the 81 measurement

973 points; **SWC**, soil water content; **Grass**, percentage of the soil surface covered by grass; **Slope**,

974 micro-topography of the terrain within the study stand; **MeanD**, mean distance from the

975 European beech trees to the 81 measurement points.

45

1　　**Spatial variability of soil respiration (R$_s$) and its controls are subjected to strong**

2　　**seasonality in an even-aged European beech (*Fagus sylvatica* L.) stand**

3

4　　**Running Title:** Space-Time R$_s$ variability in European beech stand

5

6　　**Authors**: Hereş Ana-Maria[1,2], Bragă Cosmin[3], Petritan Any Mary[3], Petritan Ion Catalin[4], Curiel

7　　Yuste Jorge[2,5,*]

8

9　　[1]Transilvania University of Braşov, Faculty of Silviculture and Forest Engineering, Department

10　　of Forest Sciences, Șirul Beethoven -1, 500123, Braşov, Romania

11

12　　[2]BC3 - Basque Centre for Climate Change, Scientific Campus of the University of the Basque

13　　Country, 48940 Leioa, Spain

14

15　　[3]National Institute for Research and Development in Forestry "Marin Drăcea", Bulevardul

16　　Eroilor 128, 077190, Voluntari, Romania

17

18　　[4]Transilvania University of Braşov, Faculty of Silviculture and Forest Engineering, Department

19　　of Forest Engineering, Forest Management Planning and Terrestrial Measurements, Șirul

20　　Beethoven -1, 500123, Braşov, Romania

21

22　　[5]IKERBASQUE - Basque Foundation for Science, Plaza Euskadi 5, 48009, Bilbao, Spain

23

24　　* Corresponding author:

25　　Dr. Jorge Curiel Yuste

26   Ikerbasque Research Professor

27   BC3 - Basque Centre for Climate Change, Sede Building 1, 1st floor, Scientific Campus of

28   the University of the Basque Country, 48940 Leioa

29   Email address: jorge.curiel@bc3research.org

30   Contact phone: +34 94-401 46 90 ext. 179

31   **Keywords:** European beech, even-aged stand, micro-topography, seasonality, soil

32   microclimate, soil respiration, spatial variability

33

34   **Abbreviations: R_s,** soil respiration; **T_s,** soil temperature; **SWC,** soil water content; **BA,** basal

35   area of the European beech trees surrounding the 81 measurement points; **SOC,** soil organic

36   carbon content; **Litter,** thickness of the litter layer; **Slope,** micro-topography of the terrain

37   within the study stand; **N_{trees},** the count of all the surrounding European beech trees around each

38   of the 81 measurement points; **DBH,** average diameter at breast height (i.e., > 6 cm) of the

39   European beech trees surrounding the 81 measurement points; **MeanD,** mean distance from the

40   European beech trees to the 81 measurement points; **Grass,** percentage of the soil surface

41   covered by grass; **Seedlings,** percentage of the soil surface covered by tree seedlings.

42 **Abstract**

43

44 Uncertainties arising from the so far poorly explained spatial variability of soil respiration (R_s)

45 remain large. This is partly due to the limited understanding on how actually spatially variable

46 R_s is, but also on how environmental controls determine R_s's spatial variability and how these

47 controls vary in time (e.g., seasonally). Our study was designed to deepen into the complexity

48 of R_s's spatial variability in a European beech even-aged stand, covering both phenologicaly

49 and climatically contrasting periods (spring, summer, autumn, winter). Although we studied a

50 relatively homogenous stand, we found a large spatial variability of R_s (coefficients of variation

51 > 30%) characterized by strong seasonality. This large spatial variability of R_s suggests that

52 even in relatively homogenous stands there is a large potential source of error when estimating

53 R_s. This was also reflected by the sampling effort needed to obtain seasonal robust estimates of

54 R_s, which may actually require a number of samples above that used in R_s studies. We further

55 postulate that the effect of seasonality on the spatial variability and environmental controls of

56 R_s was determined by the seasonal shifts of its microclimatic controls: during winter, low

57 temperatures constrain plant and soil metabolic activities and hence reduce R_s variability

58 (temperature-controlled processes), while during summer, water demand by vegetation and

59 changes in water availability due to the micro-topography of the terrain (i.e., slope) increase R_s

60 variability (water-controlled processes). This study provides novel information on the spatio-

61 temporal variability of R_s and deepens into the seasonality of its environmental controls and the

62 architecture of their causal-effect relationships controlling R_s's spatial variability. Our study

63 further shows that improving current estimates of R_s at local and regional levels might be

64 necessary in order to reduce uncertainties and improve CO_2 estimates at larger spatial scales.

65

66 **Highlights**

67

68 ❖ The spatial variability of soil respiration (R_s) and its environmental controls vary

69   seasonally

70 ❖ Seasonal shifts from temperature- to water-controlled processes determine R_s's spatial

71   variability

72 ❖ Besides microclimate, slope and grass cover explain the spatio-temporal variability of

73   R_s

74 ❖ An intense sampling effort is needed to obtaining robust R_s estimates even in

75   homogenous forests

76

77   **1. Introduction**

78

79   Soil respiration (R_s), i.e., the production and subsequent emission of carbon dioxide (CO_2) from

80   the soil to the atmosphere, is one of the key processes contributing to the global terrestrial

81   carbon (C) balance/budget. R_s is mainly produced by biological sources from the aerobic

82   respiration of decomposers (i.e., heterotrophic respiration), as well as by plant roots and

83   associated microorganisms living in the rhizosphere (i.e., autotrophic respiration) (Rodeghiero

84   & Cescatti, 2008), but also by non-biological chemical oxidation reactions of C in organic

85   matter, although at lower rates in this latter case (Raich & Schlesinger, 1992). Globally, the R_s

86   emissions amount to a total of almost 80 PgC y^{-1}, being the second largest C flux after CO_2

87   uptake by plants (Raich & Tufekciogul, 2000), which means more than half of an ecosystem's

88   total CO_2 emissions come from R_s (Barba et al., 2018; Curiel Yuste et al., 2005; Janssens et al.,

89   2001). However, R_s is also probably the least well understood part of the C budget at global

90   terrestrial ecosystems' level, based primarily on the fact that the large spatio-temporal

91   variability that characterizes this large flux requires of a substantial monitoring effort at

92   different scales and hence, of a large investment in instrumentation for its correct monitoring

93   (Bond-Lamberty & Thomson, 2010). Therefore, and despite the large critical mass of studies

94   performed to understand it (Bond-Lamberty & Thomson, 2010), our knowledge on the

95   mechanisms controlling this large flux remains very limited (e.g., Barba et al., 2013; Curiel

96   Yuste et al., 2019). Hence, there is still a need for studies designed to explore the spatio-

97   temporal variability of R_s in order to be able to calibrate models and improve predictions of soil

98   biological CO_2 emissions in a changing environment.

99

100   The magnitude of R_s-related CO_2 emissions varies in time and space depending on multiple

101   drivers. A critical mass of studies has been designed to understand how the temporal variability

102   of R_s relates to different environmental factors such as soil temperature (T_s; e.g., Chen et al.,

103   2014; Davidson et al., 1998; Epron et al., 2004*a*), soil water content (SWC; e.g., Davidson et

104   al., 2000; Oishi et al., 2013; Poblador et al., 2017), wind (e.g., Sánchez-Cañete et al., 2016), or

105   the photosynthetic activity of the plants (e.g., Bahn et al., 2009; Curiel Yuste et al., 2005;

106   Davidson et al., 1998). Nevertheless, it is important to highlight the discrepancy between the

107   large number of studies undertaken to understand the large, but predominantly explained

108   variability in time (generally seasonal) of soil CO_2 fluxes (see for instance Bond-Lamberty &

109   Thomson, 2010) and the relatively few studies undertaken to understand the enormous, but

110   largely unexplained spatial variability of this very same flux. Several studies have proposed

111   different factors that define local conditions as controls of the spatial variability of R_s at the

112   mesoscale (scale of m). Most of these studies agree on the important role of variables such as:

113   *i*). the spatial variability of soil moisture (Barba et al., 2013; Kosugi et al., 2007; Poblador et

114   al., 2017); *ii*). the structure of the overstorey plant community (Barba et al., 2013; Epron et al.,

115   2004*b*; Law et al., 2001; Saiz et al., 2006; Søe & Buchmann, 2005); *iii*). variables directly

116   related to the structure of the aboveground plant community, such as leaf production (Oishi et

117   al., 2013), root density or biomass (Knohl et al., 2008), microbial biomass, and litter thickness

118   (Hanson et al., 1993); *iv*). the quantity and quality of soil organic matter (Rayment & Jarvis,

119   2000); or *v*). the C/N ratio and bulk density of the top soil (Khomik et al., 2006; Ngao et al.,

120   2012; Saiz et al., 2006). Other topographical aspects, such as the slope and the position within

121   the landscape, have been however less studied although their contribution to explain the spatial

122   variability of R_s might also be critical (Arias-Navarro et al., 2017; Berryman et al., 2015; Brito

123   et al., 2010; Hanson et al., 1993; Riveros-Iregui et al., 2012;). All studies, nevertheless,

124   conclude that our capacity to predict the spatial variability of R_s and its environmental controls

125   remains largely insufficient (e.g., Allaire et al., 2012).

126

127   The environmental controls of the spatial variability of R_s may also vary temporally, though, to

128   the best of our knowledge, only few studies have been designed to deepen in this potential

129   temporal axis of the spatial variation of R_s (Epron et al., 2004*b*; Khomik et al., 2006; Kosugi et

130   al., 2007; Saiz et al., 2006; Shi et al., 2016; Søe & Buchmann, 2005). The complexity of the

131   spatial variability of R_s can vary seasonally (Riveros-Iregui et al., 2012; Shi et al., 2016; Søe &

132   Buchmann, 2005) specially because different environmental drivers may differently influence

133   R_s depending on the season. For instance, the influence of water availability on the spatial

134   patterns of R_s at the landscape-scale can exhibit a bidirectional behaviour, R_s being more

135   sensitive to water availability during dry periods or in highly drained areas than during wetter

136   periods or in low drainage areas (Riveros-Iregui et al., 2012). Likewise, the biomass and

137   respiration of the autotrophic (roots and rhizosphere microorganism) and heterotrophic

138   (microbial activity) components of R_s may vary in space and time depending on the

139   phenological state of the vegetation and its nutrient and water demands (Barba et al., 2013; Søe

140   & Buchmann, 2005). For this reason, understanding the drivers controlling the spatial

141   variability of R_s at different temporal scales may help us to improve and modulate the sampling

142   effort needed in order to obtain confident estimates of R_s. This also means that obtaining reliable

143   integrative measures of R_s would require different sampling efforts throughout the year. It is,

144   therefore, important to understand this seasonally-dependent complexity if we want to improve

145   our knowledge on the sampling effort needed to get accurate and costly efficient estimates of

146   R_s (Barba et al., 2013; Herbst et al., 2009; Rayment & Jarvis, 2000; Rodeghiero & Cescatti,

147   2008).

148

149   We studied the spatio-temporal variability of soil respiration (R_s) in a 4.0 ha (i.e., 200 m x 200

150   m) European beech (*Fagus sylvatica* L.) even-aged stand. Specifically, we focused on

151   understanding the potential seasonal (i.e., spring, summer, autumn, winter) variations of R_s and

152   its environmental controls to: (1) determine the magnitude of their spatial variability and the

153   sampling effort needed per each season (i.e., spring, summer, autumn, winter) to obtain robust

154   average estimates of R_s; and (2) identify the main environmental controls and the architecture

155   of their potential causal-effect relationships controlling the spatial variability of R_s along the

156   seasons (i.e., during phenologically and climatically contrasted periods of the year). We

157   hypothesized that, given the generally large influence of the aboveground plant distribution in

158   explaining the spatial variability of R_s, the spatial variability of R_s will be low in our European

159   beech even-aged study stand where trees are homogeneously distributed (H1). However, we

160   also hypothesized that, along with other already well-studied and known factors, other factors

161   (i.e., more spatially variable at stand level), such as the micro-topography of the terrain (i.e.,

162   slope) or the spatial distribution of the grass cover, will also play an important, indirect control

163   over R_s due to their influence on the spatial variability of the soil water content (SWC) (H2).

164   Finally, we also hypothesized that the predictive power of the different environmental controls

165   of the spatial variability of R_s will vary throughout the year depending on the environmental

166   constrains that act on R_s within a given season (e.g., soil temperature, T_s; or soil water content,

167   SWC) (H3).

168

169   **2. Materials and Methods**

170

171   *2.1.   Study site and stand*

172

173   The study site (i.e., forest) is located in the central-southern part of Romania, in Mihaesti (Arges

174   county; 45°05'11.8019"N, 25°03'58.0428"E), at an altitude of 570 m a.s.l. (Figure 1). This forest

175   is largely dominated by European beech, although other tree species may also be found:

176   hornbeam (*Carpinus betulus* L.)*, sessile oak *(Quercus petraea* (Matt.) Liebl.), or sweet cherry

9

177 *(Prunus avium L.)*. The density within the whole forest located in Mihaesti is of 504 trees ha^{-1},

178 with a total volume of 502 m^3 ha^{-1}, and a basal area of 33 m^2 ha^{-1} (Mihaesti Forest Management

179 Plan). Within this forest, we focused on a 4.0 ha European beech study stand (200 m x 200 m)

180 (Figure 1). The European beech trees within the study stand are mainly adult and dominant (i.e.,

181 canopy level). According to the Mihaesti Forest Management Plan, most individuals within the

182 study stand have an estimated age of ~ 85 years, which allows us to consider this study stand

183 as being even-aged. The area where our study stand is located is characterized by a temperate

184 continental climate, with a mean annual precipitation of ~ 875.21 mm, and a mean air

185 temperature of ~ 6.31°C, respectively (estimates calculated for the 1901 – 2019 period; CRU

186 TS v.4; Harris et al., 2020). The mean annual precipitation for 2016 and 2017 (i.e., the years

187 when our measurements were performed; see below) was of ~ 991.80 mm and ~ 959.60 mm,

188 respectively. As for the mean annual air temperature, it was of ~ 7.59 °C in 2016 and of 7.54

189 °C in 2017 (CRU TS v.4; Harris et al., 2020). The soils are Eutric Cambisols (clay loam)

190 covered with mull type humus, developed on a sandstone with marls parental material (Florea

191 & Munteanu, 2012). The slope within the study stand is smooth and there are no important

192 differences regarding the altitude between the upper part of the study stand and the lower part

193 of the study stand (Figure 1, small panel). Mean pH values range from 4.8 (0-10 cm soil depth)

194 to 5.2 (11-20 cm soil depth) (WTW pH330i; WTW GmbH, Weilheim, Germany).

195

196   *2.2.   Field soil respiration (R_s) and microclimatic factors measurements*

197

198 The 4.0 ha selected study stand was divided into regular 25 m x 25 m squares (Figure 1, small

199 panel). Soil respiration (R_s) measurements were then performed at each of the four corners of

200 each of the 25 m x 25 m squares, resulting thus on a total of 81 measurement points. R_s

201 measurements were all performed using a Portable Infrared Gas Analyzer (IRGA) connected to

202   a soil respiration standard chamber (EGM-4 and SRC-1; PP Systems, Amesbury, MA, USA).

203   The soil respiration chamber covered a soil surface area of 78 cm^2 and an enclosed volume of

204   1171 cm^3. Since some studies have shown a clear correlation between insertion depth, the

205   amount of cut roots, and the lost soil effluxes (Silvola et al., 1996; Wang et al., 2005), no collars

206   were inserted in the soil (Arias-Navaro et al., 2017; Epron et al., 2004b; Hanson et al., 1993;

207   Maestre & Cortina, 2003; Poblador et al., 2017). Instead, we followed a similar procedure to

208   the one described by Epron et al., 2004b and we inserted the edge of the respiration chamber to

209   a depth of 1 cm into the soil, including the litter layer. Nevertheless, this was done only after

210   firstly removing the herbaceous layer in order to avoid potential confounding effects of the

211   vegetation on R_s measurements. Furthermore, to avoid potential gas leaks due to the shallow

212   insertion of the respiration chamber (1 cm into the soil) with respect to a relatively thick low-

213   density litter layer (average 3.3 cm; Table 1), the respiration chamber was strongly pressed

214   against the soil (i.e., with the help of one hand) over the whole time measurements were

215   performed. Final R_s values were estimated for 120 seconds based on the linear increase of the

216   CO_2 concentration within the soil respiration chamber (i.e., a closed dynamic system). Soil CO_2

217   efflux measurements were always performed between 9 a.m. and 5 p.m. Additionally, the CO_2

218   effluxes were never measured during rainy days. Specifically, in case of heavy rains (i.e., > 15

219   mm), field R_s measurements were postponed 36 h to avoid the "Birch effect" (Birch, 1958).

220

221   Simultaneously to the field R_s measurements, microclimatic measurements (i.e., soil

222   temperature and the volumetric soil water content) were also performed at the same 81

223   measurement points. Specifically, soil temperature (T_s) was measured at 5 cm soil depth using

224   the STP-2 Soil Temperature Probe that was attached to the IRGA (PP Systems, Amesbury, MA,

225   USA). As for the volumetric soil water content (SWC), this variable was measured at 20 cm

226   soil depth using the TDR 300 soil moisture meter (Spectrum Technologies, Inc., Plainfield, IL,

227   USA). All field measurements (i.e., R_s, T_s, and SWC) spanned over a period of one complete

228   year and thus over the four seasons: spring (May 2016), summer (August 2016), autumn

229   (November 2016), and winter (February 2017). Within each of the 4 seasons and at each of the

230   81 measurement points, we performed 3 independent measurements for each of the 3 variables

231   (i.e., R_s, T_s, and SWC) and then averaged their corresponding values. In order to systematically

232   perform R_s, T_s, and SWC measurements at exactly the same locations within the study stand,

233   we marked the 81 measurement points with wood sticks that were maintained in their positions

234   over the whole study period. Due to the large number of measurement points (i.e., 81) and thus

235   to the considerable field effort and logistics that were needed, R_s, T_s, and SWC measurements

236   were always performed during 2 consecutive days during each season.

237

238   *2.3.   Forest structural and soil variables and the micro-topography of the terrain*

239

240   At each of the 81 measurement points, soil samples were also collected to determine the soil

241   organic carbon (SOC) content. All soil samples were collected in February 2017 after all

242   seasonal measurements (i.e., R_s, T_s, and SWC) were finished. Soil sampling was performed

243   using a metallic cylinder (5 cm diameter, and 20 cm depth) and consisted in extracting one soil

244   core at each of the 81 measurement points. SOC of the upper 20 cm of the soil profile was

245   determined through the dry combustion method using a CHNS organic elemental micro-

246   analyser (TruSpec Micro CHNS elemental analyser, LECO, New York, USA).

247

248   The thickness of the litter layer (hereinafter referred to as "litter" to simplify) was used as a

249   proxy of litter biomass, which could not be measured due to logistics. The litter, at each of the

250   81 measurement points, was measured only once during the 2016 summer, two weeks before

251   the R_s, T_s, and SWC measurements started. Although, we acknowledge the fact that it would

12

252   have been better to measure the litter layer over the year (i.e., seasons), this was not possible

253   due to logistics. Instead, we assumed that the place where there was more accumulated litter

254   (i.e., at some point) would be the same place where more litter usually falls and the opposite

255   for the places where there was less accumulated litter. Accordingly, the litter depth would be

256   basically stable over the year (i.e., seasons). Simultaneously to the litter measurements, the

257   micro-topography of the terrain (hereinafter referred to as "slope" to simplify), at each of the

258   81 measurement points, was also measured.

259

260   In order to account for the impact of the surrounding vegetation on our field measurements (i.e.,

261   within a radius of 7 m around each of the 81 measurement points), we counted all the

262   surrounding European beech trees (N_{trees}) and we measured their diameter at breast height

263   (DBH; at standard 1.3 m above from the ground) and their distance to the 81 sampling points.

264   The 7 m radius was established considering the average crown diameter of the European beech

265   trees found within the 4.0 ha study stand (Mihaesti Forest Management Plan). The DBH of the

266   trees was measured using a calliper (Haglöf, Sweden), only European beech trees with a DBH

267   > 6 cm being finally considered for this study. The measured distances were used to calculate

268   the mean distances (MeanD) from surrounding European beech trees to the 81 measurement

269   points. In order to estimate the basal area (BA; m^2 ha^{-1}) of all European beech trees with a DBH

270   > 6 cm, we calculated the sum of all their cross-sectional areas at breast height. Finally, within

271   the same radius of 7 m around each of the 81 measurement points, we also estimated the

272   percentage (%) of the soil surface covered by grass and the percentage (%) of the soil surface

273   covered by all tree seedlings. These estimations were done visually and agreed between several

274   observers for data consistency.

275

276   *2.4.   Statistical analyses*

277

278   We used different statistics (i.e., mean, M; standard deviation, SD; and relative variability, RV)

279   to estimate relative rates of spatial variability of forest structural and soil variables (i.e., BA,

280   SOC, litter, N_{trees}, DBH, MeanD, % of grass, and % of seedlings) and of the micro-topography

281   of the terrain (i.e., slope). We used the same statistics (i.e., mean, M; standard deviation, SD;

282   and relative variability, RV) plus the absolute amplitude (A; defined as the difference between

283   maximum and minimum values) to estimate relative and absolute rates of spatial variability of

284   the microclimate (i.e., T_s and SWC) and soil respiration (R_s) variables. As most studies give the

285   coefficient of variation (CV), we also calculated this statistic (i.e., expressed as a percentage)

286   for the R_s variable alone and used it to compare our results with those published in previous

287   studies. For the T_s, SWC, and R_s variables, all the above mentioned statistics were calculated

288   considering both the four seasons separately and the four seasons combined (i.e., annual). The

289   relative variability statistic (i.e., RV) was calculated following Lewontin 1966 and Webster

290   2001 as the standard deviation of the logarithms (i.e., log10 in our case) of measurements.

291   Relative variability allows thus to compare variations between different groups of observations

292   (Lewontin 1966; Webster 2001).

293

294   In order to calculate the minimum number of measurements (i.e., N) needed to obtain robust

295   estimates of R_s for each season (i.e., spring, summer, autumn, and winter), we used the

296   following power equation (Davidson et al., 2002):

297

298    $$N = [(t \times s)/(range/2)]^2 \qquad equation\ 1$$

299

300   where, t is represented by the critical value of the t-distribution (two-tailed test) for a given

301   confidence level (99, 95, and 90%, respectively) and for 80 degrees of freedom; s is the standard

14

302   deviation of all spatially independent R_s measurements per each season (i.e., spring, summer,

303   autumn, and winter); and *range* is the width of the desired interval around the mean of the R_s

304   measurements of each season (i.e., spring, summer, autumn, and winter) in which a smaller

305   sample mean is expected to fall (i.e., error limit of 10%, 20%, and 30% of the R_s measurements

306   mean per each season).

307

308   We run geostatistical analyses (i.e., experimental (semi-) variograms and theoretical

309   variograms) to determine the spatial autocorrelation of: *i*). the T_s, SWC, and R_s variables,

310   separately for each season (i.e., spring, summer, autumn, and winter); *ii*). all forest structural

311   and soil variables (i.e., basal area, BA; soil organic carbon content, SOC; thickness of the litter

312   layer, litter; number of trees surrounding the 81 measurement points, N_{trees}; diameter at breast

313   height, DBH; mean distance from surrounding European beech trees to the 81 measurement

314   points, MeanD; percentages of grass and seedlings cover around the 81 measurement points);

315   and *iii*). the micro-topography of the terrain (i.e., slope). Specifically, the experimental (semi-)

316   variograms (i.e., binned) were performed using the "variog" function available from the "geoR"

317   R package (Ribeiro et al., 2020) based on classical estimators. Further on, the theoretical

318   variograms were performed using the "likfit" function available from the "geoR" R package

319   (Ribeiro et al., 2020). These analyses were run considering the restricted maximum likelihood

320   (REML) parameter estimation, different trends (i.e., the mean part of the model; constant, first

321   order polynomial, and second order polynomial), and functions (i.e., models for the correlation

322   function; matern, exponential, Gaussian, spherical, circular, cubic, wave, powered exponential,

323   Cauchy, gneiting, and pure nugget). A total of 693 models were run. The selection of the best

324   models for each of the analysed variables was based on AIC (Akaike Information Criteria). The

325   selected models were then used to perform ordinary kriging using the "krige.conv" function

326   available from the "geoR" R package (Ribeiro et al., 2020). The "image" function available

327 from the "geoR" R package (Ribeiro et al., 2020) was finally used to visualize the spatial

328 prediction based on the fixed covariance parameters. All selected models were validated using

329 the "xvalid" function available from the "geoR" R package (Ribeiro et al., 2020).

330

331 To evaluate the microclimatic controls of the spatio-temporal variability of R_s, we run multiple

332 regression functions using the "nls" function available from the "MASS" R package (Venables

333 & Ripley, 2020). These functions were designed according to literature (i.e., Vicca et al., 2014).

334 Briefly, different models were designed to represent the independent controls of soil

335 temperature (T_s) and soil water content (SWC) on R_s, but also taking into account potential

336 unimodal responses of R_s to both microclimatic factors. R_s data was log transformed prior to

337 analyses as it did not meet the normality assumption.

338

$$\log(R_s) \sim a + b*T_s \qquad\qquad equation\ 2$$

$$\log(R_s) \sim a + b*SWC \qquad\qquad equation\ 3$$

$$\log(R_s) \sim a + b*T_s + c*T_s^2 \qquad\qquad equation\ 4$$

$$\log(R_s) \sim a + b*SWC + c*SWC^2 \qquad\qquad equation\ 5$$

$$\log(R_s) \sim a + b*T_s + c*SWC \qquad\qquad equation\ 6$$

$$\log(R_s) \sim a + b*T_s + c*SWC + d*T_s^2 \qquad\qquad equation\ 7$$

$$\log(R_s) \sim a + b*T_s + c*SWC + d*SWC^2 \qquad\qquad equation\ 8$$

339

340 Where, *a*, *b*, *c*, and *d* letters stand for coefficients of the multiple regression functions. The co-

341 variance and multicollinearity between T_s and SWC were examined prior to analyses using the

342 Variance Inflation Factor (VIF). Since the VIF was lower than 2, both microclimatic variables

343 could be used within the same model (Zuur et al., 2010). The selection of the best model was

344 based on the AIC (Akaike Information Criterion). For these analyses, the T_s, SWC, and R_s

16

345　　variables were combined over the four seasons (i.e., spring, summer, autumn, and winter). All

346　　these analyses were conducted based on the assumption that the residuals of the models were

347　　normally distributed (p > 0.05) and independent. As the assumption of independence may be

348　　justified when data collection has been performed based on a probability sampling design (e.g.,

349　　de Gruijter et al., 2006) and our data collection has been performed based on a grid sampling

350　　design, we acknowledge the fact that the spatial auto-correlation between data at nearby

351　　measurement points might impact some of the obtained results.

352

353　　To describe potential complex causal-effect relationships that might determine the spatio-

354　　temporal variability patterns of R_s, we run Structural Equation Models (SEMs). SEMs analyses

355　　allowed to test for the direct and indirect effects of all our measured in the field variables (i.e.,

356　　microclimatic variables, forest structural and soil variables, and the micro-topography of the

357　　terrain) on seasonal (i.e., spring, summer, autumn, and winter) R_s. SEMs analyses were carried

358　　out using the "psem" function available from the "piecewiseSEM" R package (Lefcheck, 2016).

359　　To harmonize the results of the SEMs with those obtained from the multiple regression

360　　functions analyses, R_s was logarithmically transformed prior to analyses. Separated SEMs were

361　　built for each of the four seasons (i.e., spring, summer, autumn, and winter). All SEMs were

362　　designed based on hypotheses supported on simple univariate correlations between the different

363　　microclimatic (i.e., soil temperature, T_s; soil water content, SWC), micro-topography of the

364　　terrain (i.e., slope), soil (i.e., soil organic carbon content, SOC; and litter), and forest structural

365　　(i.e., basal area, BA; number of trees, N_{trees}; diameter at breast height, DBH; mean distance,

366　　MeanD; % of grass; and % of seedlings) variables (i.e., predictor variables). Furthermore, their

367　　potential complex causal-effect relationships, that might determine the spatio-temporal

368　　variability of R_s, were also considered. To test the goodness of fit of the SEMs, the Fisher's C

369　　statistic was calculated. The Fisher's C statistic follows a chi-squared distribution and tests if

370   the model fits the data ($p > 0.05$) or not ($p < 0.05$). Several SEMs were run, the selection of the

371   best one being based on the AIC (Akaike Information Criteria) (Lefcheck, 2016).

372   All statistical analyses were carried out in R (v. 4.0.0, R Core Team, 2020). Statistical

373   relationships were considered significant at $p < 0.05$.

374

375   **3. Results**

376

377   *3.1.*   *The spatial variability of the forest structural and soil variables around the 81*

378   *soil respiration (R_s) measurement points*

379

380   We found a relatively low spatial variability (i.e., expressed here as relative variability, RV;

381   Table 1) for forest structural variables such as DBH (RV = 0.1) and MeanD (RV = 0.1) (Table

382   1, Figure S1). Similar results were obtained also for soil variables such as SOC (RV = 0.1) and

383   litter (RV = 0.1) (Table 1, Figure S1). On the other hand, the spatial variability of the understory

384   vegetation (i.e., % of grass and % of seedlings) showed the highest values and was higher

385   relative to the spatial variability of the overstorey vegetation (i.e., BA and N_{trees}) (Table 1,

386   Figure S1). High spatial variability values were found also for the slope (RV = 0.3) (Table 1,

387   Figure S1).

388

Statistics	BA (m² ha⁻¹)	SOC (t ha⁻¹)	Litter (cm)	Slope (%)	N_{trees} (N ha⁻¹)	DBH (cm)	MeanD (m)	Grass (%)	Seedlings (%)
M	47.3	44.3	3.3	12.2	443	32.8	3.5	57.5	9.1
SD	16.9	12.9	0.7	8.3	200	6.3	0.8	31.1	8.6
RV	0.2	0.1	0.1	0.3	0.2	0.1	0.1	0.4	0.3

389   **Table 1.** Mean (M), standard deviation (SD), and relative variability (RV; following Lewontin

390   1966 and Webster 2001) values of forest structural, soil, and the micro-topography of the terrain

391   variables. *Where*, **BA**, basal area of the European beech trees surrounding the 81 measurement

392   points; **SOC**, soil organic carbon content; **Litter**, thickness of the litter layer; **Slope**, micro-

393   topography of the terrain within the study stand; N_{trees}, the count of all the surrounding

394   European beech trees around each of the 81 measurement points; **DBH**, average diameter at

395   breast height (i.e., > 6 cm) of the European beech trees surrounding the 81 measurement points;

396   **MeanD**, mean distance from the European beech trees to the 81 measurement points; **Grass**,

397   percentage of the soil surface covered by grass; **Seedlings**, percentage of the soil surface

398   covered by tree seedlings.

399

400   *3.2.   Soil respiration (R_s) sampling effort needed per season*

401

402   The calculation of the minimum number of measurements needed to obtain robust estimates of

403   R_s for each season (i.e., spring, summer, autumn, and winter) showed how sensitive *equation 1*

404   was to both the error limit (i.e., 10%, 20%, and 30%) and the confidence interval (90%, 95%,

405   and 99%) (Table S1). Accordinly, the calculated sampling effort varied within and among

406   seasons depending on the error limit and the confidence interval. Specifically, the sampling

407   effort varied more strongly within seasons than among them (Table S1). As for the sampling

408   effort needed from one season to another to obtain robust estimates of R_s, differences were not

409   so strong especially between summer, autumn, and winter (Table S1). Spring was the season

410   when less minimum R_s measurements seem to be needed to obtain robust estimates of R_s (Table

411   S1) no matter the confidence level and the error limit (Table S1). On the other hand, winter was

412   found to be the season when more sampling effort seems to be needed to obtain robust estimates

413   of R_s no matter the confidence level and the error limit (Table S1). The sampling effort for the

19

414   summer season seems to be quite close to the winter one, while the sampling effort for the

415   autumn season was found to be slightly lower (i.e., in between the spring and summer), no

416   matter the confidence level and the error limit (Table S1).

417

418   *3.3.   Seasonal and spatial variability of soil respiration (R_s), soil temperature (T_s),*

419   *and soil water content (SWC)*

420

421   As expected, both microclimatic variables (i.e., T_s and SWC) experienced very different

422   seasonal patterns during the study period (Table 2, Figure 2). On one hand, T_s experienced large

423   seasonal changes, peaking during summer and reaching its minimums during winter (Table 2,

424   Figure 2a). On the other hand, values of SWC experienced less seasonality, reaching its

425   minimums during summer, but being very stable and similar for the rest of the year (Table 2,

426   Figure 2b). Seasonality of R_s followed a pattern similar to that observed for T_s, peaking during

427   both spring and summer, and reaching its minimums during winter (Table 2, Figure 2c).

428

429   The spatial variability of the microclimatic variables was also markedly different (Table 2,

430   Figure 3). Specifically, the spatial variability of T_s was generally smaller (RV values ranging

431   from 0.01 to 0.10), within the range of 3.1 to 5.3 ºC of amplitude (Table 2, Figure 3A, D, G, J),

432   than the spatial variability of SWC (RV values ranging from 0.10 to 0.14), within the range of

433   31.9 to 54.6 % vol. of amplitude (Table 2, Figure 3B, E, H, K). R_s was the variable with the

434   highest spatial variability (RV values ranging from 0.13 to 0.17), within the range of 2.5 to 11.9

435   $\mu mol\ CO_2\ m^{-2}\ s^{-1}$ of amplitude (Table 2, Figure 3C, F, I, L) and coefficients of variation above

436   30% (Table 2). As concerning the standard deviation of the mean values, both T_s and SWC

437   showed seasonal changes, summer being the season that showed the lowest values (Table 2).

438   Standard deviation values for R_s also showed seasonal changes, being higher in spring and

439   summer and smaller in winter (Table 2), a pattern that followed the increase of the R_s rates

440   (Figure 2).

441

Period	T_s (°C)				SWC (% vol.)				R_s ($\mu mol\ CO_2\ m^{-2}\ s^{-1}$)				
	M	SD	RV	A	M	SD	RV	A	M	SD	RV	CV	A
Spring	14.4	0.9	0.03	4.6	33.0	10.2	0.14	54.6	6.3	2.0	0.13	31.1	8.7
Summer	17.4	0.6	0.01	3.1	24.9	6.6	0.12	31.9	6.4	2.4	0.17	37.6	11.9
Autumn	7.5	0.7	0.04	3.9	29.6	8.1	0.11	42.7	2.8	1.0	0.15	34.9	4.8
Winter	3.8	0.9	0.10	5.3	33.9	8.0	0.10	41.9	1.3	0.5	0.16	36.4	2.5
Annual	10.8	5.5	0.27	17.7	30.4	9.0	0.13	54.6	4.2	2.7	0.33	65.1	13.6

442   **Table 2.** Mean (M), standard deviation (SD), relative variability (RV; following Lewontin 1966

443   and Webster 2001), Coefficient of Variation (CV; only for the R_s variable) expressed as a

444   percentage, and absolute amplitude (A; defined as the difference between maximum and

445   minimum values) values of soil microclimate (i.e., T_s, soil temperature; and SWC, soil water

446   content) and soil respiration (R_s) measurements. The above mentioned statistics have been

447   calculated both at the seasonal level (i.e., spring, summer, autumn, and winter) and over the

448   four seasons combined (i.e., annual).

449

450   *3.4. The spatio-temporal variability of soil respiration (Rs)*

451

452   The model that best explained the microclimatic controls over the spatio-temporal variability

453   of R_s was the model that considered unimodal responses of R_s to T_s and a negative linear

454   response of R_s to SWC (i.e., equation 7) (Table S2, Figure 4). Specifically, the unimodal effect

455   of T_s on R_s translated into a seasonal sensitivity of R_s to T_s: i.e., R_s response to T_s was stronger

456   at lower T_s values (i.e., corresponding to autumn and winter seasons) than at higher T_s values

457   (i.e., corresponding to spring and summer seasons) (Figure 4a) when R_s reached its peak (Table

458   2) and its response to the seasonal changes of T_s was low. The overall effect of SWC over the

459   spatio-temporal variability of R_s was negative, this response being evidenced by the negative

460   slope of this relationship (Figure 4b). This negative effect was further on highlighted by the

461   overall relationship that was found between SWC and R_s at the spatial scale (i.e., results of the

462   SEM analyses), where higher values of SWC were generally associated with low R_s rates (see

463   Figures 4b and 5). Hence, the SWC effect on R_s was mainly driven by the spatially net negative

464   effect of SWC on R_s.

465

466   Both multiple regression functions and SEMs agreed that the microclimatic variables (T_s and

467   SWC; Figures 4 and 5) were, overall, the most important factors controlling the variability of

468   R_s in our 4.0 ha study stand. Nevertheless, SEMs further showed how the architecture of the

469   potential causal-effect relationships controlling R_s's spatial variability increased in complexity

470   (Figure 5) during spring and summer, when the spatial variability of R_s was maximal (see SD

471   and A in Table 2 and Figure 2C). Specifically, SEMs highlighted how during the summer

472   season, when the spatial variability of R_s was the highest (Table 2), the number of variables

473   ultimately involved in controlling the spatio-temporal variability of R_s were also high compared

474   to, e.g. winter or autumn (Figure 5). Also, the predictive capacity of the spatio-temporal

475   variability of R_s varied seasonally (Table 3), the coefficient of determination (R^2) ranging from

476   0.10 in winter to 0.29 in autumn. SEMs showed how both the forest structural (N_{trees}, MeanD,

477   and % of grass cover) and the micro-topography of the terrain (i.e., slope) variables may

478   strongly influence, directly and indirectly the spatio-temporal variability of R_s (Figure 5).

479   Specifically, in spring and summer, the % of grass cover was negatively associated with T_s and

480   SWC, which on their turn exerted a further positive and negative, respectively, influence on the

481   spatio-temporal variability of R_s (Figure 5). N_{trees} instead, always showed a direct and positive

22

482   effect on the spatio-temporal variability of R_s during the coldest seasons (i.e., autumn and

483   winter; Figure 5). The slope (i.e., the micro-topography of the terrain within the study stand)

484   was negatively related with MeanD in spring and summer, this relationship being especially

485   important during summer when MeanD exerted some control (i.e., positive relationship) over

486   R_s (Figure 5).

Season	Response	Predictor	Estimate	SE	df	p-value	SRW	Response	R²	n	Fisher's C	df	p-value
	R_s	T_s	0.0583	0.0154	78	0.0003	0.39	R_s	0.17	81	10.193	10	0.424
Spring	R_s	Slope	-0.0031	0.0017	78	0.0672	-0.19	MeanD	0.05				
	MeanD	Slope	-0.0213	0.0103	79	0.0413	-0.23	T_s	0.07				
	T_s	Grass	-0.0076	0.0031	79	0.0170	-0.26						
	R_s	SWC	-0.0086	0.0028	76	0.0030	-0.32	R_s	0.24	80	12.3	12	0.422
	R_s	T_s	-0.0836	0.0320	76	0.0109	-0.27	SWC	0.11				
Summer	R_s	MeanD	0.0471	0.0227	76	0.0412	0.22	MeanD	0.05				
	SWC	Slope	-0.1890	0.0829	77	0.0253	-0.25						
	SWC	Grass	-0.0571	0.0226	77	0.0134	-0.28						
	MeanD	Slope	-0.0213	0.0103	79	0.0413	-0.23						
	R_s	T_s	0.0504	0.0233	77	0.0331	0.22	R_s	0.29	81	1.581	2	0.454
Autumn	R_s	SWC	-0.0076	0.0018	77	0.0001	-0.40	T_s	0.07				
	R_s	N_{trees}	0.0002	0.0001	77	0.0486	0.20						
	T_s	N_{trees}	0.0008	0.0004	79	0.0190	0.26						
Winter	R_s	N_{trees}	0.0003	0.0001	79	0.0045	0.31	R_s	0.10	81	0	0	1

487

24

488 **Table 3.** Statistics of the Structural Equation Models (SEMs) analyses showing causal-effect relationships that determine the spatio-temporal

489 variability of soil respiration (R_s). Only significant ($p < 0.05$) and marginally significant ($p < 0.1$) causal relationships are given. *Where*, **T_s**, soil

490 temperature; **SWC**, soil water content; **Slope**, micro-topography of the terrain within the study stand; **N_{trees}**, the count of all surrounding European

491 beech trees around each of the 81 measurement points; **MeanD**, mean distance from the European beech trees to the 81 measurement points; **Grass**,

492 percentage of the soil surface covered by grass; **SE**, standard error; **df**, degrees of freedom; **SRW**, Standardized Regression Weights; **R^2**, the

493 coefficient of determination; **n**, sampling size; **Fisher's C statistic**, follows a chi-squared distribution and tests if the model fits the data ($p > 0.05$)

494 or not ($p < 0.05$). The right hand part of the table shows the statistics of the best models representing the spatio-temporal variability of R_s during

495 each of the four different seasons (i.e., spring, summer, autumn, and winter).

496

497   **4.   Discussion**

498

499   We here report high soil respiration (R_s) coefficient of variation values (i.e., CV, ranging from

500   31.1 in spring to 37.6 in summer; see Table 2) in an even-aged European beech study stand

501   located in the central-southern part of Romania (Mihaesti, Arges county). These values are

502   higher or comparable to other CV values mentioned in previous studies (e.g., Barba et al., 2013;

503   Epron et al., 2004*b*; Kosugi et al., 2007; Ngao et al., 2012; Shi et al., 2016; Stoyan et al., 2000),

504   although caution should be taken when comparing CV values among studies as they might also

505   vary depending on the considered spatial scales (e.g., Darenova & Čater, 2020; Ngao et al.,

506   2012). Nevertheless, independent of this consideration, the high CV values we obtained here

507   refute our first hypotheses (H1). In fact, the magnitude of the spatial variability of R_s during the

508   warmest seasons (i.e., spring and summer) was comparable to the overall annual variability of

509   R_s (see SD and A values in Table 2), which reinforces the idea of the large, though generally

510   neglected, impact of R_s's spatial variability on estimates of soil CO_2 effluxes, even in

511   homogenous ecosystems such as the European beech even-aged study stand that we considered

512   here. The calculated large sampling effort needed to obtain robust estimates of R_s for any given

513   season (being even larger in winter, see Table S1) further highlights the importance of the

514   spatial variability of R_s as a potential source of uncertainty on local and global CO_2 estimates

515   and that should be taken into account. This is of upmost importance especially now, when the

516   number of studies dedicated to scale up CO_2 observations from local to global levels is growing.

517   Accordingly, our study suggests that obtaining robust estimates of R_s at the local level may

518   require of more intense spatial sampling efforts, than those generally carried out for logistical

519   reasons, in order to address and diagnose uncertainties on CO_2 estimates at the global level

520   (e.g., Jian et al., 2018; Warner et al., 2019).

521

522　　The large spatio-temporal variability of R_s was strongly and directly determined by soil

523　　microclimatic conditions (T_s and SWC; Figures 4 and 5). Nevertheless, as hypothesized (H2),

524　　less considered variables such as the forest structural ones (i.e., grass, MeanD, N_{trees}) or the

525　　micro-topography of the terrain (i.e., slope), proved to have a determinant, direct or indirect,

526　　effect on the observed spatio-temporal variability of R_s. In the case of the slope and the grass

527　　cover variables, they both showed further tight relationships with soil microclimatic conditions

528　　(i.e., T_s and SWC). These relationships were found to be significant in spring and summer

529　　(Figure 5), the two seasons when R_s values peaked (Table 2). Specifically, grass cover

530　　modulated the T_s variable in spring, with an indirect effect over R_s. In summer instead, when

531　　SWC usually registers low values and the competition for water and nutrients between the

532　　heterotrophic communities and the vegetation is high (Villegas et al., 2010), grass cover

533　　modulated the SWC availability, with an indirect effect over R_s. Our results highlight thus the

534　　importance of seldom considered variables, such as the micro-topography of the terrain (e.g.,

535　　Arias-Navarro et al., 2017) and the vegetation (e.g., Søe & Buchmann, 2005), in R_s studies, as

536　　they may actually substantially impact, either directly or indirectly, the spatio-temporal

537　　variability of R_s. Instead, in our European beech even-aged study stand, we found no significant

538　　effects of variables generally well associated with the spatial variability of R_s, such as the litter

539　　(e.g., Epron et al., 2004*b*; Katayama et al., 2009; Saiz et al., 2006) or the soil organic carbon

540　　content (e.g., Søe & Buchmann, 2005). Although the fact that litter thickness was only

541　　measured once (i.e., during the 2016 summer; cf. 2.3. section), and thus may have generated a

542　　certain source of noise in our models (since the litter generally accumulates in autumn in

543　　deciduous-dominated forests), we assumed that our summer measurements contain very

544　　valuable information on the long-term spatial patterns of litter accumulation on the soil, and

545　　therefore, valuable information on where litter can have a greater impact on the spatial

546　　variability of soil processes in the long term. We are further aware of the limitations of our

27

study, since other variables, such as soil compaction (Schwen et al., 2015) or the spatial

distribution of the root biomass (Søe & Buchmann, 2005), that have not been measured, may

have also helped to explain the observed spatial patterns of R_s. However, we expect that effects

of the spatial variability of soil compaction on, e.g. water infiltration or CO_2 diffusivity (e.g.,

Schwen et al., 2015), will not be as high as in more intensively used stands since our study

stand has not undergone any forestry intervention during the last 85 years and has no livestock

load (according to the Mihaesti Forest Management Plan). On the other hand, and given the

logistical inability to obtain estimates of the spatial distribution of root biomass, our exhaustive

characterization of the distribution of trees and understorey (e.g., grass and seedlings) around

the 81 measurement points emerged as a good proxy highly associated with the distribution of

roots, assuming that proximity to vegetation is closely associated with root density in the soil

(Søe & Buchmann, 2005).

Our results further emphasized the importance of understanding the temporal (i.e., seasonal)

changes in the magnitude and controls of spatial variability of R_s. This variability could be

especially important in temperate areas where microclimatic conditions (i.e., T_s and SWC), soil

CO_2 effluxes, and vegetation activity may vary dramatically throughout the year (e.g., Curiel

Yuste et al., 2005). Indeed, and also as hypothesized (H3), our results indicated that, along with

the observed seasonal variability in the magnitude of R_s, the variables that control the spatial

variability of R_s were also subjected to strong seasonality. The architecture of the causal-effect

relationships controlling R_s's spatial variability varied between the four seasons and showed an

increased complexity during spring and summer, while in autumn and especially in winter these

relationships were much simpler (Figure 5). In line with these findings, spring and summer

were also the seasons when the highest R_s values were registered, as expected for temperate

ecosystems (e.g., Knohl et al., 2008; Saiz et al., 2006; Shi et al., 2016; Søe & Buchmann, 2005).

572   These high R_s values coincided thus with the warmest temperatures of the year, with the peak

573   in plant and soil biological activity, and with the highest variability of R_s in absolute terms.

574   These results are of upmost importance as they highlight the fact that in order to obtain robust

575   estimates of R_s-CO_2 derived emissions and to have a deeper understanding on the R_s variability,

576   both spatial and temporal R_s controlling processes need to be taken into account.

577

578   Based on our results, we postulate that in this even-aged European beech study stand, the

579   observed spatio-temporal changes and controls of the R_s respond to a seasonal shift that goes

580   from temperature-controlled (i.e., winter and autumn) to water-controlled (i.e., spring and

581   summer) processes. Figure 6 shows a conceptual framework, based on our results, that

582   illustrates this shift in time. During cold periods, when the seasonal variability of R_s was, as

583   expected in a temperature forest (e.g., Curiel Yuste et al. 2003), strongly limited by T_s (Figure

584   4a), the spatial variability in R_s followed the low spatial variability of T_s (represented as

585   standard deviation of the mean R_s or T_s in Figure 6), resulting in low spatial variability of R_s

586   (Table 2, Figure 6). Most factors had insignificant effects over the spatial variability of R_s

587   during the winter season, when only N_{trees} (i.e., the number of European beech trees surrounding

588   the 81 measurement points) showed a positive relationship with R_s (Figure 5). These results

589   might be related with a larger autotrophic respiration contribution to R_s during winter when

590   European beech trees are able to maintain part of their fine root biomass alive (e.g., Büttner and

591   Leuschner, 1994; Zwetsloot et al., 2019). A similar result was found for the autumn season,

592   when N_{trees} also showed a positive relationship with R_s (Figure 5). During warm periods (i.e.,

593   summer), when the soil metabolic activity is at its peak (reflected in higher rates of R_s; Table

594   2, Figure 2), the increase in temperature and vegetation activity increases the demand for SWC

595   (evapotranspiration), which then becomes a limiting factor for R_s. Although our SWC

596   measurements were too deep (i.e., 20 cm soil depth) to capture this increasing water control

29

597   (i.e., our model could not capture a positive effect of SWC on R_s; see Figure 4b), this seasonal

598   water limitation of R_s was evidenced by the low sensitivity to temperature that R_s experienced

599   during the warmer periods (Figure 4a), which is the shape typically observed when R_s responds

600   to a shift that goes from temperature-controlled to water-controlled processes (e.g., Curiel-

601   Yuste et al., 2003, 2005; Davidson & Janssens, 2006). This shift towards R_s's spatial variability

602   being water-controlled resulted in an increase in R_s variability, which subsequently become

603   more spatially variable than temperature (reflected in increased standard deviation values of R_s

604   with respect to T_s; see Figure 6). The shift towards a water-limited R_s system that generated

605   spatial variability of R_s (Figure 6) also increased the complexity of R_s controls (Figures 5 and

606   6). This is because the increase in vegetation activity triggered a higher competition for water,

607   as evidenced by, e.g. the strong negative influence of tree proximity (i.e., positive effect of

608   MeanD in summer on R_s; Figure 5) or the strong negative effect of the grass cover over SWC

609   during summer (Figure 5). Hence, the evaporative demand of the vegetation (i.e., MeanD and

610   grass cover) exerted direct and indirect controls over the spatial variability of R_s during dry,

611   warm, and phenologically active periods (i.e., spring and summer), contributing to an increase

612   in the spatial variability of R_s. The slope (i.e., the micro-topography of the terrain) was another

613   variable that contributed, directly and indirectly, to the increase in the spatial variability of R_s

614   during warmer periods characterized by higher water demand (Figure 5). Slope may have large

615   impacts over water availability and water balances by creating spatial variability in e.g. the

616   incidence of solar radiation at the floor level and water run-off (Berryman et al., 2015; Riveros-

617   Iregui et al., 2012), with further consequences on soil CO_2 effluxes, even across short distances

618   (Arias-Navarro et al., 2017). It is likely that, at our study stand, the spatial distribution of the

619   slopes captured the spatial variability of SWC during drier periods (i.e., summer) better than

620   our own SWC measurements taken at 20 cm depth. This is because during periods of high water

621   demand (i.e., summer), SWC decreases very fast in the uppermost layer of the soil, where most

622   of both autotrophic and heterotrophic activities concentrate (Curiel Yuste et al., 2003, 2005),

623   whereas at 20 cm depth SWC remains above the volumetric content thresholds at which SWC

624   limits Rs, as stated by the fact that no positive relationship was found between SWC and R_s

625   (Figures 4b and 5).

626

627   **5. Conclusions**

628

629   We here highlight the fact that the spatial variability of R_s proves to be high even in a relatively

630   homogenous even-aged European beech study stand of 4.0 ha. Accordingly, our estimates

631   regarding the sampling effort needed to obtain robust estimates of R_s further suggest that most

632   studies to date might have probably underestimated the sampling effort needed to obtain

633   accurate spatial estimates of R_s throughout the year. Our study further shows that the spatial

634   variability of R_s, varied significantly throughout the year, peaking in spring and summer and

635   being low in winter, coinciding thus with the seasonal variability in the absolute magnitude of

636   R_s. We here postulate that in this European beech-dominated even-aged study stand, the

637   observed large seasonal changes in the magnitude and controls of the spatial variability of R_s

638   respond to a seasonal shift that goes from temperature-controlled (i.e., winter and autumn) to

639   water-controlled (i.e., spring and summer) processes. This is because when temperatures and

640   water demands are high, the evaporative demand of both the overstorey but also the understorey

641   vegetation, as well as the micro-topography of the terrain (i.e., slope), generate spatial

642   complexity in soil R_s. During winter, temperature limits processes and prevents most other

643   factors from spatially influencing R_s. In conclusion, obtaining robust, accurate estimates of R_s-

644   derived CO_2 effluxes, may profit from: (1) a deeper understanding of how the spatial patterns

645   of R_s varies across seasons, e.g., understanding when processes shift from being controlled by

646   temperature (i.e., winter and autumn) to being controlled by water (i.e., spring and summer);

647   and (2) a deeper understanding on how, when, and where, factors such as the micro-topography

648   of the terrain or the plant-plant and the plant-soil competition for water may contribute to this

649   spatial variability of R_s. In line with our findings, it would be interesting to test in future at

650   which extent this observed trends apply to other types of ecosystems or if they may also be

651   extrapolated to latitudinal and/or altitudinal gradients, i.e., whether R_s's spatial complexity may

652   increase considering gradients that go from temperature-limited (e.g., temperate) to water-

653   limited (e.g., arid and semi-arid) systems, or from topographically simple (e.g., valleys) to

654   topographically more complex (e.g., mountains) systems.

655

656   **Acknowledgements**

657

667

References

Allaire, S.E., Lange, S.F., Lafond, J.A., Pelletier, B., Cambouris, A.N. & Dutilleul P. (2012). Multiscale spatial variability of CO_2 emissions and correlations with physico-chemical soil properties. *Geoderma*, 170, 251-260. https://doi.org/10.1016/j.geoderma.2011.11.019

Arias-Navarro, C., Díaz-Pinés, E., Klatt, S., Brandt, P., Rufino, M.C., Butterbach-Bahl, K. & Verchot, L.V. (2017). Spatial variability of soil N_2O and CO_2 fluxes in different topographic positions in a tropical montane forest in Kenya. *Journal of Geophysical Research: Biogeosciences*, 122, 514-527. https://doi.org/10.1002/2016JG003667

Bahn, M., Reichstein, M., Davidson, E.A., Grünzweig, J., Jung, M., Carbone, M.S., Epron, D., Misson, L., Nouvellon, Y., Roupsard, O., Savage, K., Trumbore, S.E., Gimeno. C., Curiel Yuste, J., Tang, J., Vargas, R. & Janssens, I.A. (2009). Soil respiration at mean annual temperature predicts annual total across vegetation types and biomes. *Biogeosciences*, 7, 2147-2157. 10.5194/bg-7-2147-2010

Barba, J., Cueva, A., Bahn, M., Barron-Gafford, G.A., Bond-Lamberty, B., Hanson, P.J., Jaimes, A., Kulmala, L., Pumpanen, J., Scott, R.L., Wohlfahrt, G. & Vargas, R. (2018). Comparing ecosystem and soil respiration: Review and key challenges of tower-based and soil measurements. *Agricultural and Forest Meteorology*, 249, 434-443. https://doi.org/10.1016/j.agrformet.2017.10.028

Barba, J., Curiel Yuste, J., Martínez-Vilalta, J. & Lloret, F. (2013). Drought-induced tree species replacement is reflected in the spatial variability of soil respiration in a mixed

692 Mediterranean forest. *Forest Ecology and Management*, *306*, 79-87.

693 https://doi.org/10.1016/j.foreco.2013.06.025

694

695 Berryman, E.M., Barnard, H.R., Adams, H.R., Burns, M.A., Gallo, E. & Brooks, P.D. (2015).

696 Complex terrain alters temperature and moisture limitations of forest soil respiration across a

697 semiarid to subalpine gradient. *Journal of Geophysical Research: Biogeosciences*, 120, 707-

698 723. https://doi.org/10.1002/2014JG002802

699

700 Birch, H.F. (1958). The effect of soil drying on humus decomposition and nitrogen availability.

701 *Plant and Soil*, 10, 9-31. https://doi.org/10.1007/BF01343734

702

703 Bond-Lamberty, B. & Thomson, A. (2010). Temperature-associated increases in the global soil

704 respiration record. *Nature*, 464, 579-582. https://doi.org/10.1038/nature08930

705

706 Brito, L.F., Marques Júnior, J., Pereira, G.T. & La Scala Junior, N. (2010). Spatial variability

707 of soil CO_2 emission in different topographic positions. *Bragantia*, 69, 19-27.

708 http://dx.doi.org/10.1590/S0006-87052010000500004

709

710 Büttner, V. & Leuschner, C. (1994). Spatial and temporal patterns of fine root abundance in a

711 mixed oak-beech forest. *Forest Ecology and Management*, 70, 11–21.

712 https://doi.org/10.1016/0378-1127(94)90071-X

713

714 Chen, S., Zou, J., Hu, Z., Chen, H. & Lu, Y. (2014). Global annual soil respiration in relation

715 to climate, soil properties and vegetation characteristics: Summary of available

716   data. *Agricultural   and   Forest   Meteorology*, 198-199,   335-346.

717   https://doi.org/10.1016/j.agrformet.2014.08.020

718

719   Curiel Yuste J., Janssens, I.A., Carrara, A., Meiresonne, L. & Ceulemans, R. (2003). Interactive

720   effects of temperature and precipitation on soil respiration in a temperate maritime pine forest.

721   *Tree Physiology*, 23, 1263-1270. https://doi.org/10.1093/treephys/23.18.1263

722

723   Curiel Yuste, J., Nagy, M., Janssens, I.A., Carrara, A. & Ceulemans, R. (2005). Soil respiration

724   in a mixed temperate forest and its contribution to total ecosystem respiration. *Tree Physiology*,

725   25, 609-619. https://doi.org/10.1093/treephys/25.5.609

726

727   Curiel Yuste, J., Flores-Rentería, D., García-Angulo, D., Hereş, A.-M., Bragă, C., Petritan, A.-

728   M. & Petritan, I.C. (2019). Cascading effects associated with climate-change-induced conifer

729   mortality in mountain temperate forests result in hot-spots of soil CO_2 emissions. *Soil Biology*

730   *& Biochemistry*, 133, 50-59. https://doi.org/10.1016/j.soilbio.2019.02.017

731

732   Darenova, E. & Čater, M. (2020). Effect of spatial scale and harvest on heterogeneity of forest

733   floor CO_2 efflux   in   a   sessile   oak   forest.   *Catena*,   188,   104455,

734   https://doi.org/10.1016/j.catena.2020.104455

735

736   Davidson, E.A., Belk, E. & Boone, R.D. (1998). Soil water content and temperature as

737   independent or confounded factors controlling soil respiration in a temperate mixed hardwood

738   forest. *Global Change Biology*, 4, 217-227. https://doi.org/10.1046/j.1365-2486.1998.00128.x

739

740   Davidson, E.A., Verchot, L.V., Cattânio, J.H., Ackerman, I.L. & Carvalho, J.E.M. (2000).

741   Effects of soil water content on soil respiration in forests and cattle pastures of eastern

742   Amazonia. *Biogeochemistry*, 48, 53-69. https://doi.org/10.1023/A:1006204113917

743

744   Davidson, E.A., Savage, K., Verchot, L.V. & Navarro, R. (2002). Minimizing artifacts and

745   biases in chamber-based measurements of soil respiration. *Agricultural and Forest*

746   *Meteorology*, 113, 21-37. https://doi.org/10.1016/S0168-1923(02)00100-4

747

748   Davidson, E.A. & Janssens, I.A. (2006). Temperature sensitivity of soil carbon decomposition

749   and feedbacks to climate change. *Nature*, 440, 165-173. https://doi.org/10.1038/nature04514

750

751   de Gruijter, J., Brus, D.J., Bierkens, M.F.P. & Knotters, M. (2006). Sampling for Natural

752   Resource Monitoring. Springer-Verlag Berlin Heidelberg. 10.1007/3-540-33161-1

753

754   Epron, D., Ngao, J. & Granier, A. (2004*a*). Interannual variation of soil respiration in a beech

755   forest ecosystem over a six-year study. *Annals of Forest Science*, 61, 499-505.

756   https://doi.org/10.1051/forest:2004044

757

758   Epron, D., Nouvellon, Y., Roupsard, O., Mouvondy, W., Mabiala, A., Saint-André, L., Joffre,

759   R., Jourdan, C., Bonnefond, J.-M., Berbigier, P. & Hamel, O. (2004*b*). Spatial and temporal

760   variations of soil respiration in a *Eucalyptus* plantation in Congo. *Forest Ecology and*

761   *Management*, 202, 149-160. https://doi.org/10.1016/j.foreco.2004.07.019

762

763   Florea, N. & Munteanu, I. (2012). Sistemul Roman de Taxonomie a Solurilor – SRTS (in

764   Romanian). Editura Sitech, Craiova, Romania.

36

765

766   Hanson, P.J., Wullschleger, S.D., Bohlman, S.A. & Todd, D.E. (1993). Seasonal and

767   topographic patterns of forest floor CO_2 efflux from an upland oak forest. *Tree Physiology*, 13,

768   1-15. https://doi.org/10.1093/treephys/13.1.1

769

770   Harris, I., Osborn, T.J., Jones, P., Lister, D., 2020. Version 4 of the CRU TS monthly high-

771   resolution gridded multivariate climate dataset. Scientific Data 7, 109.

772   https://doi.org/10.1038/s41597-020-0453-3.

773

774   Herbst, M., Prolingheuer, N., Graf, A., Huisman, J.A., Weihermüller, L. & Vanderborght, J.

775   (2009). Characterization and understanding of bare soil respiration spatial variability at plot

776   scale. *Vadose Zone Journal*, 8, 762-771. https://doi.org/10.2136/vzj2008.0068

777

778   Janssens, I.A., Lankreijer, H., Matteucci, G., Kowalski, A.S., Buchmann, N., Epron, D.,

779   Pilegaard, K., Kutsch, W., Longdoz, B., Grünwald, T., Montagnani, L., Dore, S., Rebmann, C.,

780   Moors, E.J., Grelle, A., Rannik, Ü., Morgenstern, K., Oltchev, S., Clement, R., Guðmundsson,

781   J., Minerbi, S., Berbigier, P., Ibrom, A., Moncrieff, J., Aubinet, M., Bernhofer, C., Jensen, N.O.,

782   Vesala, T., Granier, A., Schulze, E.D., Lindroth, A., Dolman, A.J., Jarvis, P.G., Ceulemans, R.

783   & Valentini, R. (2001). Productivity overshadows temperature in determining soil and

784   ecosystem respiration across European forests. *Global Change Biology*, 7, 269-278.

785   https://doi.org/10.1046/j.1365-2486.2001.00412.x

786

787   Jian, J., Steele, M.K., Thomas, R.Q., Day, S.D. & Hodges, S.C. (2018). Constraining estimates

788   of global soil respiration by quantifying sources of variability. *Global Change Biology*, 24,

789   4143– 4159. https://doi.org/10.1111/gcb.14301

37

790

791 Katayama, A., Kume, T., Komatsu, H., Ohashi, M., Nakagawa, M., Yamashita, M., Otsuki, K.,

792 Suzuli, M. & Kumagai, T. O. (2009). Effect of forest structure on the spatial variation in soil

793 respiration in a Bornean tropical rainforest. *Agricultural and Forest Meteorology*, 149, 1666-

794 1673. https://doi.org/10.1016/j.agrformet.2009.05.007

795

796 Khomik, M., Arain, M.A. & McCaughey, J.H. (2006). Temporal and spatial variability of soil

797 respiration in a boreal mixedwood forest. *Agricultural and Forest Meteorology*, 140, 244-256.

798 https://doi.org/10.1016/j.agrformet.2006.08.006

799

800 Kosugi, Y., Mitani, T., Itoh, M., Noguchi, S., Tani, M., Matsuo, N., Takanashi, S., Ohkubo, S.

801 & Nik, A.R. (2007). Spatial and temporal variation in soil respiration in a Southeast Asian

802 tropical rainforest. *Agricultural and Forest Meteorology*, 147, 35-47.

803 https://doi.org/10.1016/j.agrformet.2007.06.005

804

805 Knohl, A., Søe, A.R.B., Kutsch, W.L., Göckede, M. & Buchmann, N. (2008). Representative

806 estimates of soil and ecosystem respiration in an old beech forest. *Plant and Soil*, 302, 189-202.

807 https://doi.org/10.1007/s11104-007-9467-2

808

809 Law, B.E., Kelliher, F.M., Baldocchi, D.D., Anthoni, P.M., Irvine, J., Moore, D. & Van Tuyl,

810 S. (2001). Spatial and temporal variation in respiration in a young ponderosa pine forest during

811 a summer drought. *Agricultural and Forest Meteorology*, 110, 27-43.

812 https://doi.org/10.1016/S0168-1923(01)00279-9

813

814   Lefcheck, J.S. (2016). piecewiseSEM: Piecewise structural equation modelling in R for

815   ecology, evolution, and systematics. *Methods in Ecololgy Evolution*, 7, 573-579.

816   https://doi.org/10.1111/2041-210X.12512

817

818   Lewontin, R.C. (1966). On the Measurement of Relative Variability. *Systematic Biology*, 15,

819   141-142. https://doi.org/10.2307/sysbio/15.2.141

820

821   Maestre, F.T. & Cortina, J. (2003). Small-scale spatial variation in soil CO_2 efflux in a

822   Mediterranean   semiarid   steppe. *Applied   Soil   Ecology*, 23,   199-209.

823   https://doi.org/10.1016/S0929-1393(03)00050-7

824

825   Ngao, J., Epron, D., Delpierre, N., Bréda, N., Granier, A. & Longdoz, B. (2012). Spatial

826   variability of soil CO_2 efflux linked to soil parameters and ecosystem characteristics in a

827   temperate beech forest. *Agricultural and Forest Meteorology*, 154-155, 134-146.

828   https://doi.org/10.1016/j.agrformet.2011.11.003

829

830   Oishi, A.C., Palmroth, S., Butnor, J.R., Johnsen, K. & Oren, R. (2013). Spatial and temporal

831   variability of soil CO_2 efflux in three proximate temperate forest ecosystems. *Agricultural and*

832   *Forest Meteorology*, 171-172, 256-269. https://doi.org/10.1016/j.agrformet.2012.12.007

833

834   Poblador, S., Lupon, A., Sabaté, S. & Sabater, F. (2017). Soil water content drives

835   spatiotemporal patterns of CO_2 and N_2O emissions from a Mediterranean riparian forest

836   soil. *Biogeosciences*, 14, 4195-4208. https://doi.org/10.5194/bg-14-4195-2017

837

838 R Core Team (2020). R (v. 4.0.0, 2020): A language and environment for statistical computing.

839 R Foundation for Statistical Computing, Vienna, Austria. URL http://www.R-project.org/

840

841 Raich, J.W. & Schlesinger, W.H. (1992). The global carbon dioxide flux in soil respiration and

842 its relationship to vegetation and climate. *Tellus B: Chemical and Physical Meteorology*, 44,

843 81-99. https://doi.org/10.3402/tellusb.v44i2.15428

844

845 Raich, J.W. & Tufekcioglu, A. (2000). Vegetation and soil respiration: Correlation and controls.

846 *Biogeochemistry*, 48, 71-90. https://doi.org/10.1023/A:1006112000616

847

848 Rayment, M.B. & Jarvis, P.G. (2000). Temporal and spatial variation of soil CO_2 efflux in a

849 Canadian boreal forest. *Soil Biology & Biochemistry*, 32, 35-45. https://doi.org/10.1016/S0038-

850 0717(99)00110-8

851

852 Ribeiro Jr., P.J., Diggle, P.J., Schlather, M., Bivand, R. & Ripley, B. (2020). geoR: Analysis of

853 Geostatistical Data. R package version 1.8-1. https://CRAN.R-project.org/package=geoR

854

855 Riveros-Iregui, D.A., McGlynn, B.L., Emanuel, R.E. & Epstein, H.E. (2012). Complex terrain

856 leads to bidirectional responses of soil respiration to inter-annual water availability. *Global

857 Change Biology*, 18, 749-756. https://doi.org/10.1111/j.1365-2486.2011.02556.x

858

859 Rodeghiero, M. & Cescatti, A. (2008). Spatial variability and optimal sampling strategy of soil

860 respiration. *Forest   Ecology   and   Management*, 255,   106-112.

861 https://doi.org/10.1016/j.foreco.2007.08.025

862

863   Saiz, G., Green, C., Butterbach-Bahl, K., Kiese, R., Avitabile, V. & Farrell, E.P. (2006).

864   Seasonal and spatial variability of soil respiration in four Sitka spruce stands. *Plant and*

865   *Soil*, 287, 161-176. https://doi.org/10.1007/s11104-006-9052-0

866

867   Shi, B., Gao, W., Cai, H. & Jin, G. (2016). Spatial variation of soil respiration is linked to the

868   forest structure and soil parameters in an old-growth mixed broadleaved-Korean pine forest in

869   northeastern China. *Plant and Soil*, 400, 263-274. https://doi.org/10.1007/s11104-015-2730-z

870

871   Silvola, J., Alm, J., Ahlholm, U., Nykanen, H., & Martikainen, P.J. (1996). CO_2 fluxes from

872   peat in boreal mires under varying temperature and moisture conditions. *Journal of Ecology*,

873   219-228. https://www.jdoi.org./10.2307/2261357

874

875   Søe, A.R.B. & Buchmann, N. (2005). Spatial and temporal variations in soil respiration in

876   relation to stand structure and soil parameters in an unmanaged beech forest. *Tree*

877   *Physiology*, 25, 1427-1436. https://doi.org/10.1093/treephys/25.11.1427

878

879   Stoyan, H., De-Polli, H., Böhm, S., Robertson, G.P. & Paul, E.A. (2000). Spatial heterogeneity

880   of soil respiration and related properties at the plant scale. *Plant and Soil*, 222, 203-214.

881   https://doi.org/10.1023/A:1004757405147

882

883   Sánchez-Cañete, E.P., Oyonarte, C., Serrano-Ortiz, P., Curiel Yuste, J., Pérez-Priego, O.,

884   Domingo, F. & Kowalski, A.S. (2016). Winds induce CO_2 exchange with the atmosphere and

885   vadose zone transport in a karstic ecosystem. *Journal of Geophysical Research:*

886   *Biogeosciences*, 121, 2049-2063. https://doi.org/10.1002/2016JG003500

887

888   Schwen, A., Jeitler, E. & Böttcher, J. (2015). Spatial and temporal variability of soil gas

889   diffusivity, its scaling and relevance for soil respiration under different tillage. *Geoderma*, 259-

890   260, 323-336. https://doi.org/10.1016/j.geoderma.2015.04.020

891

892   Venables, W.N. & Ripley, B.D. (2002). Modern Applied Statistics with S, Fourth edition.

893   Springer, New York. ISBN 0-387-95457-0, http://www.stats.ox.ac.uk/pub/MASS4/

894

895   Vicca, S., Bahn, M., Estiarte, M., van Loon, E.E., Vargas, R., Alberti, G., Ambus, P., Arain, M.

896   A., Beier, C., Bentley, L. P., Borken, W., Buchmann, N., Collins, S.L., de Dato, G., Dukes, J.

897   S., Escolar, C., Fay, P., Guidolotti, G., Hanson, P. J., Kahmen, A., Kröel-Dulay, G., Ladreiter-

898   Knauss, T., Larsen, K. S., Lellei-Kovacs, E., Lebrija-Trejos, E., Maestre, F.T., Marhan, S.,

899   Marshall, M., Meir, P., Miao, Y., Muhr, J., Niklaus, P.A., Ogaya, R., Peñuelas, J., Poll, C.,

900   Rustad, L.E., Savage, K., Schindlbacher, A., Schmidt, I.K., Smith, A.R., Sotta, E.D., Suseela,

901   V., Tietema, A., van Gestel, N., van Straaten, O., Wan, S., Weber, U. & Janssens, I. A. (2014).

902   Can current moisture responses predict soil CO_2 efflux under altered precipitation regimes? A

903   synthesis   of   manipulation   experiments.   *Biogeosciences*,   11,   2991-3013.

904   https://doi.org/10.5194/bg-11-2991-2014

905

906   Villegas, J. C., D. D. Breshears, C. B. Zou, and P. D. Royer. (2010). Seasonally Pulsed

907   Heterogeneity in Microclimate: Phenology and Cover Effects along Deciduous Grassland–

908   Forest Continuum. *Vadose Zone Journal*, 9, 537-547. https://doi.org/10.2136/vzj2009.0032

909

910   Wang, W.J., Zu, Y.G., Wang, H.M., Hirano, T., Takagi, K., Sasa, K. & Koike, T. (2005). Effect

911   of collar insertion on soil respiration in a larch forest measured with a LI-6400 soil CO_2 flux

912   system. *Journal of Forest Research*, 10, 57-60. https://doi.org/10.1007/s10310-004-0102-2

913

914 Warner, D.L., Bond-Lamberty, B., Jian, J., Stell, E. & Vargas, R. (2019). Spatial predictions

915 and associated uncertainty of annual soil respiration at the global scale. *Global Biogeochemical*

916 *Cycles*, 33, 1733– 1745. https://doi.org/10.1029/2019GB006264

917

918 Webster, R. (2001). Statistics to support soil research and their presentation. *European*

919 *Journal of Soil Science*, 52, 331-340. https://doi.org/10.1046/j.1365-2389.2001.00383.x

920

921 Zuur, A.F., Ieno, E.N. & Elphick, C.S. (2010). A protocol for data exploration to avoid common

922 statistical problems. *Methods in Ecology and Evolution*, 1, 3-14. https://doi.org/10.1111/j.2041-

923 210X.2009.00001.x

924

925 Zwetsloot, M.J., Goebel. M., Paya, A., Grams, T.E.E. & Bauerle, T.L. (2019). Specific spatio-

926 temporal dynamics of absorptive fine roots in response to neighbor species identity in a mixed

927 beech–spruce forest. *Tree Physiology*, 39, 1867-1879. https://doi.org/10.1093/treephys/tpz086

928

929 **Figure captions:**

930 **Figure 1.** Map indicating the location of Romania within Europe and the location of the study

931 site in the central-southern part of Romania (i.e., Mihaesti, Arges county). The small panel

932 shows the sampling design: a 4.0 ha (i.e., 200 m x 200 m) even-aged European beech stand

933 divided into 25 m x 25 m squares. The scale that appears on the right size of the small panel

934 indicates the altitude (m a.s.l.) gradient within the study stand.

935 **Figure 2**. Seasonal (i.e., spring, summer, autumn, and winter) patterns of: a) soil temperature

936 (T_s); b) soil water content (SWC); and c) soil respiration (R_s).

937 **Figure 3**. Spatial prediction based on the fixed covariance parameters generated by performing

938 geostatistical analyses on the seasonal (i.e.., spring, summer, autumn, and winter) spatial

939 distribution of soil temperature (T_s), soil water content (SWC), and soil respiration (R_s).

940 **Figure 4**. Representation of the best model (Table S2) that explained the microclimatic controls

941 (soil temperature, T_s; and soil water content, SWC) over the spatio-temporal variability of soil

942 respiration (R_s): a) R_s response to T_s; and b) R_s response to SWC. Black opened dots represent

943 the row data, while red (i.e., R_s response to T_s model) and blue (i.e., R_s response to SWC model)

944 opened dots represent the fitted by the best model data. To ease the interpretation, the results of

945 the multiple regression functions, for which R_s was logarithmically transformed, were back-

946 transformed to the original scale.

947 **Figure 5**. Path diagrams showing the results of the Structural Equation Models (SEMs),

948 represented by seasons. Arrows indicate causal relationships: positive and negative effects are

949 indicated by solid and dashed arrows, respectively. Only the significant ($p < 0.05$) and

950 marginally significant ($p < 0.1$) relationships were represented (see Table 3). The number given

951 next to each arrow represents the Standardized Regression Weights (SRW) values given in

952 Table 3. Path diagrams are represented in a plot where the X-axis represents the seasons (i.e.,

953 spring, summer, autumn, and winter) and the Y-axis represents the mean values of the soil

954   respiration (R_s) flux for each season. *Where*, **Grass**, percentage of the soil surface covered by

955   grass; **T_s**, soil temperature; **R_s**, soil respiration; **Slope**, micro-topography of the terrain within

956   the study stand; **MeanD**, mean distance from the European beech trees to the 81 measurement

957   points; **SWC**, soil water content; **N_{trees}**, the count of all the surrounding European beech trees

958   around each of the 81 measurement points.

959   **Figure 6.** Conceptual framework illustrating how the observed spatio-temporal changes and

960   environmental controls of the soil respiration (R_s) respond to a seasonal shift that goes from

961   temperature-controlled (i.e., winter and autumn) to water-controlled (i.e., spring and summer)

962   processes. The X-axis represents the seasonal (i.e., winter, autumn, spring, and summer) soil

963   temperature (T_s) changes. The Y-axis represents the spatial variability of soil temperature (T_s)

964   and R_s represented as the standard deviation (SD) of the mean. The path diagrams, obtained

965   from the Structural Equation Models (SEMs; Figure 5), are also represented to show how the

966   complexity of the controls of R_s increases along with the spatial variability of R_s. In the upper

967   part of the figure, the shift that goes from temperature-controlled (i.e., winter and autumn) to

968   water-controlled (i.e., spring and summer) processes over the spatial variability of R_s, is

969   indicated. The small figure panel included within the conceptual framework is represented by

970   Figure 4*a*, with the red arrows indicating the seasonal temperature control of R_s (winter and

971   autumn) and the flattening of this control during warmer periods (spring and summer). *Where*,

972   **N_{trees}**, the count of all the surrounding European beech trees around each of the 81 measurement

973   points; **SWC**, soil water content; **Grass**, percentage of the soil surface covered by grass; **Slope**,

974   micro-topography of the terrain within the study stand; **MeanD**, mean distance from the

975   European beech trees to the 81 measurement points.

Supplementary material

Season	Minimum soil respiration (R_s) measurements number (i.e., N)		
	Error limit	Confidence interval		
		90%	95%	99%
Spring	±10%	112	160	281
	±20%	28	40	70
	±30%	12	18	31
Summer	±10%	156	223	392
	±20%	39	56	98
	±30%	17	25	44
Autumn	±10%	141	202	355
	±20%	35	51	89
	±30%	16	22	39
Winter	±10%	164	234	412
	±20%	41	59	103
	±30%	18	26	46

Table S1. Minimum number of measurements (i.e., N) needed to obtain robust estimates of soil respiration (R_s) for each season (i.e., spring, summer, autumn, and winter) according to *equation 1* (cf. 2.4. Statistical analyses). Results are given for 90%, 95%, and 99% confidence intervals. The *range* is the width of the desired interval around the mean of the R_s measurements of each season (i.e., spring, summer, autumn, and winter) in which a smaller sample mean is expected to fall (i.e., error limit of 10%, 20%, and 30% of the R_s measurements mean per each season).

European Journal of Soil Science

Model	a	b	c	d	AIC	R^2
$\log(R_s) \sim a + b*T_s$	0.6002***	0.0843***			125.30	0.85
$\log(R_s) \sim a + b*SWC$	2.0141***	-0.0166***			505.55	0.27
$\log(R_s) \sim a + b*T_s + c*T_s^2$	0.1483*	0.2002***	-0.0055***		83.45	0.87
$\log(R_s) \sim a + b*SWC + c*SWC^2$	2.9595***	-0.0772***	0.0009***		491.43	0.35
$\log(R_s) \sim a + b*T_s + c*SWC$	0.7544***	0.0825***	-0.0044*		121.50	0.85
$\log(R_s) \sim a + b*T_s + c*SWC + d*T_s^2$	**0.3144***	**0.2008***	**-0.0051**	**-0.0056***	**76.76**	**0.87**
$\log(R_s) \sim a + b*T_s + c*SWC + d*SWC^2$	1.0960***	0.0812***	-0.0252**	0.0003*	117.65	0.85

Table S2. Results of multiple regression functions used to explain the spatio-temporal variability of soil respiration (R_s). The table shows the models that were considered (i.e., following Vicca et al., 2014), the estimated coefficients of the multiple regression (a, b, c, and d), the AIC (Akaike Information Criterion) values, and the coefficient of determination (R^2) values. The best model, based on AIC, is marked in bold. *Where*, superscript asterisks of the estimated coefficients of the multiple regression (i.e., a, b, c, and d) stand for: p-values < 0.05 (*), p-values < 0.01 (**), and p-values < 0.001 (***), respectively.

Figure caption:

Figure S1. Spatial prediction based on the fixed covariance parameters generated by performing geostatistical analyses on the seasonal spatial distribution of: **BA**, basal area of the European beech trees surrounding the 81 measurement points *(panel A)*; **SOC**, soil organic carbon content *(panel B)*; **Litter**, thickness of the litter layer *(panel C)*; **Slope**, micro-topography of the terrain within the study stand *(panel D)*; N_{trees}, the count of all the surrounding European beech trees around each of the 81 measurement points *(panel E)*; **DBH**, average diameter at breast height (i.e., > 6 cm) of the European beech trees surrounding the 81 measurement points *(panel F)*; **MeanD**, mean distance from the European beech trees to the 81 measurement points *(panel G)*; **Grass**, percentage of the soil surface covered by grass *(panel H)*; **Seedlings**, percentage of the soil surface covered by tree seedlings *(panel I)*.